INTERNATIONAL ATOMIC ENERGY AGENCY
UNITED NATIONS EDUCATIONAL, SCIENTIFIC AND CULTURAL ORGANIZATION

INTERNATIONAL CENTRE FOR THEORETICAL PHYSICS
34100 TRIESTE (ITALY) - P.O.B. 586 - MIRAMARE - STRADA COSTIERA 11 - TELEPHONE: 2240-1
CABLE: CENTRATOM - TELEX 460392-1

H4.SMR/204 - 39

WINTER COLLEGE ON

ATOMIC AND MOLECULAR PHYSICS

(9 March - 3 April 1987)

LASERS

S. SVANBERG

Lund Institute of Technology
S-221 00 Lund
Sweden

LASERS

Atomic and Molecular Spectroscopy
Chapter 8

In preparation for
Springer Series in Optical Sciences

Sune Svanberg
Department of Physics
Lund Institute of Technology
1987

8. LASERS

8.1. Introduction

In this chapter we will discuss the general principles of lasers and study the most important tunable lasers that are of primary spectroscopic interest. Since many tunable lasers are optically pumped by fixed-frequency lasers we will also describe the most useful types of such lasers. For a more thorough account of laser physics we refer the reader to standard textbooks [8.1-8.10].

The first operating laser, the ruby laser, was constructed in 1960 by Maiman [8.11]. An important step in the development chain resulting in the laser was a theoretical paper from 1958 by Schawlow and Townes [8.12], who analysed the prerequisites for laser action. The ammonia maser had been introduced as early as 1954 by Gordon, Zeigler and Townes [8.13]. This device operated in the microwave region and the laser is the counterpart in the visible wavelength region. As we will see, it is not trivial to bridge the large frequency gap between the microwave and optical regions. The 1964 Nobel Prize in Physics was awarded to Basov, Prokhorov and Townes for the development of the maser and the laser [8.14-16]. Maser and laser are acronyms for "microwave" and "light", respectively, "amplification by stimulated emission of radiation". The stimulated emission is essential in both processes, and we will first discuss this phenomenon. Let us, in the same way as on page .., consider a system of atoms with two energy levels E_1 and E_2 as shown in Fig. 8.1.

Fig. 8.1. here

Photons of energy E_2-E_1 are allowed to impinge on the system and we consider which of the two processes, absorption or stimulated emission, is the most probable. In Chapter 4, we showed that $B_{21}=B_{12}$ and therefore the relative probability of the two events is only dependent on the populations of the individual levels. In a system in thermodynamical equilibrium (left), the lower level is generally strongly overpopulated and therefore the photon is normally absorbed. In order to make the stimulated emission process more probable, we must in one way or another, induce a greater population

in the upper level than in the lower level. Then a greater number of photons are obtained than the number impinging on the medium. Stimulated photons have the same frequency, phase and direction of propagation as the stimulating photons and are described as coherent. We have thus shown that population inversion is a prerequisite for amplification by stimulated emission of radiation. Note the complete symmetry pertaining to the two processes of absorption and stimulated emission [2.2]. By arranging a feedback cavity around the amplifying medium a self-oscillating laser can be obtained, as will be discussed in more detail later. A complete discussion of the conditions for reaching the threshold for laser oscillation must also include considerations of linewidths.

The construction of a maser or a laser involves the fundamental task of creating a population inversion. Spontaneous emission is not desired in this case, since it reduces the population difference without leading to the emission of coherent photons. Such decays constitute noise in the amplifier that the inverted system constitutes. A good introduction to laser physics is obtained by considering the mechanism of the ammonia maser. The ammonia molecule is schematically drawn in Fig. 8.2. The nitrogen atom oscillates back and forth through the plane defined by the hydrogen atoms. Two

Fig. 8.2 here

eigenstates are possible for this inversion oscillation corresponding to a symmetric and an anti-symmetric wavefunction. The energy separation between these eigenstates corresponds to 23.87 GHz or a wavelength of 1.25 cm for absorbed/emitted photons. In Fig. 8.2 Townes' set-up is also shown (See also the hydrogen maser, p. ...). From the gas reservoir molecules emerge in both energy states. In passing an inhomogeneous electric field, molecules in the upper energy level will be focused into a cavity, while lower-level molecules are defocused and filtered away. In this process the molecular induced dipole moment is active (c.f. atomic beam magnetic resonance, p. ...). The cavity is resonant at the transition frequency between the eigenstates. An inverted population is sustained in the cavity . If a microwave signal of the correct frequency is then fed into the cavity it will give rise to stimulated emission and the signal will be amplified. If sufficiently many

molecules in the upper energy state are fed into the cavity, self-oscillation can be initiated by noise photons also present in the cavity. The ammonia maser was used as a clock before more accurate atomic clocks were developed.

Whereas amplification (oscillation) is obtained comparatively readily at these frequencies, which are of the order of 10^{10} Hz, it is considerably more difficult to achieve a corresponding situation for optical waves with a frequency of 10^{15} Hz. The reason is clear from Eq. (4.27).

$$\frac{A}{B_{12}\rho(\nu)} = \frac{8\pi h\nu^3}{c^3\rho(\nu)} \qquad (8.1)$$

i.e. the ratio between the number of spontaneous and stimulated decays increases as ν^3. Thus, the upper level will be comparatively rapidly depopulated by spontaneous decays and a very efficient pumping mechanism for the upper level is necessary to achieve laser action. From this argument it follows that it is very difficult to construct an X-ray laser. However, a great deal of research is being devoted to this problem and significant progress has already been made. In particular, amplification has been demonstrated in neon-like selenium (Se XXV) at 206 and 210 Å (3s - 2p transitions; see Fig. 8.15) following the impact of a high-energy laser pulse on a selenium foil, which then virtually explodes [8.17]. In another system amplification on the Balmer-α line in C VI (182 Å) has been obtained [8.18].

8.2 Coherence

Lasers are characterized by light that is highly coherent in comparison with light from conventional light sources. There are two types of coherence: temporal coherence and spatial coherence. The degree of temporal coherence of a light source is a measure of the possibility of predicting phase and amplitude for the light at a given location and at a certain time, provided that these quantities were known at an earlier well-defined time, at the same point. As we

discussed in Chapter 4, there is a time uncertainty, τ, associated with the spontaneous decay of an excited atom. If the classical wave approach is applied to the light, then the wave will be emitted during $\sim\tau$ seconds, and therefore the length l_c, the coherence length of the connected wave train, will be

$$l_c = \tau c \qquad (8.2)$$

Because of the finite emission time in this picture, the wave train is cut off and a Fourier analysis of the train yields a frequency spread of $\Delta\nu = 1/2\pi\tau$, as previously discussed. From a quantum-mechanical point of view the argument should be given the other way round. The time uncertainty yields a frequency spread and a corresponding associated length of the wave train. Wave trains emitted in different decays are completely unrelated. For $\tau = 10^{-8}$ s a coherence length of 3 m is obtained. Practical light sources have a Doppler broadening which is considerably larger than the natural radiation width. Because of the increased frequency spread a prediction of the phase is made more difficult. Line light sources have a typical coherence length of ~10 cm. Light sources, emitting a Planck distribution clearly have a very short coherence length.

A light wave is considered to be spatially coherent if there is a constant phase difference between different points of observation. Light that is emitted from different parts of a conventional light source is not phase-related. Therefore, the light from an extended light source will not be spatially coherent.

A good measure of the coherence of a light source is its ability to produce stable interference fringes. (An incoherent light source may produce momentary interference but the fringes continuously move swiftly and unpredictably.) The two types of coherence can be illustrated by two examples. If the path difference in a Michelson interferometer (p. xxx) is 1 m no fringes are obtained with a conventional light source because of its poor temporal coherence. If the two slits in Young's experiment are illuminated by light from different parts of a fluorescence tube no fringes are obtained because of the poor spatial coherence of the light source. Lasers

have very high temporal and spatial coherence since the photons are produced in chain reactions of stimulated emissions, in which all the generated photons represent waves with a common phase.

8.3 Resonators and Mode Structure

A population-inverted medium will amplify an incoming wave of the correct frequency through stimulated emission. Whereas the maser in the microwave region is an amplifier with a low noise level, finding applications e.g. in radio astronomy (p. xxx), a laser in the visible region is very noisy because of the increasing importance of the spontaneous emission. According to (8.1) the signal-to-background ratio will be reduced by a factor of about 10^{15} for a frequency change of a factor 10^5, from microwaves to visible light. Therefore, lasers are rarely used for light amplification, except for the case of amplifying laser pulses. Lasers are normally used as light generators (oscillators). An amplifier becomes an oscillator if feedback is introduced. This can be achieved by placing the laser medium in a resonator consisting of two mirrors (See Figs 8.1 and 8.3). A spontaneously generated noise photon of the correct

Fig. 8.3 here

frequency and direction of propagation (perpendicular to the end mirror) is amplified and starts the process. The light intensity is substantially increased by reflections back and forth through the laser medium. In order to sustain the laser action, it is necessary to continuously pump in order to maintain the population inversion. In order to obtain a useful external beam, one of the mirrors is made partially transparant. Clearly, the emerging light represents a loss factor and the degree of output coupling possible without terminating the laser action depends on the gain of the medium. Ideally, the extracted energy would be the only source of loss. By using multiple dielectric layers the absorption losses due to the mirrors can be kept well below one per cent. All optical surfaces inside the cavity must be kept very clean since any absorption is amplified by the multiple passes. In the figure the laser mirrors are indicated as plane. For such a system the alignment of the resonator is critical if losses are to be prevented. A considerably

more stable configuration is obtained if at least one of the mirrors is slightly cuired. In Fig. 8.4 a number of resonator arrangements are illustrated. The relative merits of different configurations are discussed, e.g. in Refs [8.19,8.20].

Fig. 8.4

As for a microwave cavity, several types of transverse electromagnetic oscillations or modes are possible for a laser cavity. Generally, one tries to isolate the mode that has the highest symmetry. This mode is designated TEM_{oo}. Other modes (TEM_{pq}, p, q indices) corresponding to more or less asymmetric radiation fields can be supressed by making the tube containing the laser medium sufficiently narrow or by introducing an axial aperture. A laser beam due to a laser oscillating in the TEM_{oo} mode has a symmetric cross section and the intensity falls off according to a gaussian distribution. Laser modes are discussed by Kogelnik and Li [8.21].

As a consequence of the coherence, the laser light can be transmitted as an almost parallel bundle. The small divergence is a consequence of the unavoidable influence of diffraction. For radiation in phase and with the same amplitude over a circular aperture of diameter d, the angle θ between the centre of the diffraction pattern and the first black interference ring is given by

$$\theta = 1.22\frac{\lambda}{d} \qquad (8.3)$$

A visible diffraction-limited laser with an emerging beam of diameter 1 mm will have a divergence of about 0.5 mrad. Many practical systems are diffraction-limited only. For such a laser the spot at a distance of 1 km has a diameter of about 1 m. By first expanding the beam to a larger value of d it is possible to achieve a correspondingly smaller divergence. By focusing a parallel TEM_{oo} beam a very small spot diameter can be obtained. For a perfect lens of focal length f we obtain:

$$r = f\theta \qquad (8.4)$$

A very high degree of linear polarization can be obtained for a laser with low losses in one direction of oscillation and high losses in the perpendicular direction. For a laser with a gas as the active medium this is accomplished by placing the windows of the gas container at Brewster's angle to the optical axis of the laser (Fig. 8.5). For other lasers some other type of polarizer can be placed inside the cavity.

Fig. 8.5 here

We have now discussed different characteristics of laser light without dealing with its frequency distribution in detail. It is evident that a stable oscillation mode can be achieved in the resonator only if there is constant constructive interference, i.e. standing waves. This occurs when an integer number of half wavelengths fit into the cavity of (optical) pathlength l. By considering two adjacent modes we obtain the mode separation $\Delta\nu$:

$$n\frac{\lambda}{2} = n\frac{c}{2\nu} = (n+1)\frac{c}{2(\nu+\Delta\nu)} = l \qquad (8.5)$$

$$\Delta\nu = \frac{c}{2l}$$

This expression has already been derived (p.). Clearly, the laser cavity is a Fabry-Pérot resonator with a free spectral range given by (8.5). With a cavity length of 1 m the mode separation is 150 MHz.

Let us now consider a gas laser, for which the stimulated emission occurs for a certain spectral line, determined mostly by Doppler and pressure broadening. Modes not falling within the linewidth are impossible since there is no gain for such modes. As a matter of fact, modes that are not close to the peak of the profile (the gain profile) will have too low a gain to compensate for the losses. Clearly, there is a certain threshold for the pump energy below which no modes at all have a sufficient gain. When lasing, only the most favourable modes will oscillate because of the regenerative nature of the laser action ("strong become stronger, weak become weaker"). When several modes oscillate simultaneously we talk about multi-mode operation. By introducing a Fabry-Pérot interferometer into the laser cavity with a free spectral range sufficiently large so that only one of its transmission peaks falls in the region

Fig. 8.6 here

for possible laser action, a single cavity mode can be selected (single-mode operation). The interferometer is frequently made as a plane-parallel disc with semitransparent dielectric coatings (an "etalon"). The choice of mode is made by inclining the etalon. The transmission maxima of the etalon are also influenced by the temperature. In the absence of temperature stabilization, "mode-hopping" can occur.

When the laser is oscillating in only one mode it produces a beam of very sharp frequency. Because of the generation of light by stimulated emission inside the cavity the linewidth will neither be limited by the width of the Fabry-Pérot resonance (the Airy function) nor by the natural radiation width. Using indirect measurement techniques, linewidths of the order of 1 Hz have been established for a He-Ne laser, approaching the Schawlow-Townes limit [8.12]. To obtain narrow lines a careful stabilization of the length of the laser cavity using a servo system is necessary. Otherwise vibrations will cause an considerable effective linewidth. Even without such servo stabilization a single-mode laser has very good temporal coherence. In comparison, the coherence length for a multi-mode laser is very small. A high spatial coherence is still maintained due to phase locking in the stimulated emission. Therefore, sharp interference fringes are obtained in most interference experiments.

Now we will study a number of laser types more closely. We distinguish between fixed-frequency lasers and tunable lasers. In a limited sense, the former type is also tunable since different modes under the gain curve can be selected. In lasers for which the active medium is a solid, the gain curve can be moved slightly by changing the temperature. We will primarily discuss fixed-frequency lasers that are used for the pumping of tunable lasers. By a tunable laser

we here mean a laser whose wavelength can be varied over a large region (>100 Å). Such lasers, which are of great spectroscopic interest, will be discussed in some detail.

8.4 Fixed-Frequency Lasers

8.4.1 The Ruby Laser

As we have mentioned, laser action was first observed in ruby. Ruby is a pink crystal of Al_2O_3 with an addition of about 0.05% Cr_2O_3. Only the Cr^{3+} ions are of interest here since the other ions do not participate in the process. The chromium ion has three d electrons in its unfilled shell and has a ^4F term as the groundstate term. The next higher state is a ^2G term. The ruby crystal has a weakly rhombic structure. Because of the action of the crystal field, the ^4F term will be split into the levels $^4F_1$, $^4F_2$ and $^2A_2$, where the designations are no longer the ordinary ones from atomic spectroscopy but are defined in the group-theory treatment of the crystal field problem. The ^2G term is split into levels designated $^2A_1$, $^2F_1$, $^2F_2$ and ^2E. The $^4F_1$ and $^4F_2$ levels are strongly broadened to energy bands, whereas ^2E has a doublet structure. In Fig. 8.7 the energy levels of Cr^{3+} in ruby that are relevant for laser action are indicated. The ruby crystal has strong, broad absorption bands around 550 and 400 nm. Ions that have been pumped to the ^4F bands will fall, within 10^{-7} s, to the ^2E

Fig. 8.7 here

levels, in which a population is quickly built up because the lifetime of this level is very long; about 5 ms. Population inversion with regard to the ground state is most easily achieved for the lower of the two ^2E levels. Stimulated emission is obtained at 6943 Å at room temperature. If the crystal is cooled to 77 K (liquid nitrogen temperature) the wavelength is shifted to 6934 Å. In the ruby laser, which is an example of a three-level laser, population inversion must be achieved with regard to the normally well populated ground state. It is thus necessary to pump the ions very

efficiently from the ground state to the ^4F levels. In Fig. 8.8 one possible pumping arrangement (also used by Maiman) is shown. A ruby rod, about 5 cm long and with flat, parallel silvered end surfaces,

Fig. 8.8 here

is placed inside a helical flash-lamp, filled with e.g. xenon at high pressure (See p. xxx). A capacitor of about 100 µF charged to about 2 kV is discharged through the flashlamp, which lights up for about 1 ms. Because of the broad absorption bands of ruby (see p. xxx) a non-negligible part of the light, emitted as a continuum, is absorbed. After about 0.5 ms stimulated emission is transmitted through the one semi-transparent end surface of the rod. The light is emitted as a sequence of short spikes of about 1 µs duration. This is due to the disappearance of the population inversion when stimulated emission has occurred. The flash-lamp is still on and needs some time to restore the population inversion leading to the emission of a new laser spike. This behaviour, which is frequently not wanted, can be eliminated by Q-switching. In this case, laser mirrors, separated from the rod, are used and the light path between the mirrors is initially blocked. The quality factor or Q value of the cavity is then low and stimulated emission is not initiated although a strong inversion has occurred. If the blocking is quickly removed the cavity can enhance the light field and the emission occurs in a giant pulse. In practice, polarized laser light is used and the Kerr or Pockels effect are employed to rapidly switch the plane of polarization. Giant pulses can have a peak power of 10^8 W and a pulse width of about 10 ns.

8.4.2 4-Level Lasers

We have already mentioned the difficulties involved with a three-level laser in which the laser transition is terminated in the continuously well populated ground state. The successful operation of the ruby laser relies on the very favourable combination of broad absorption bands and the long upper-state lifetime allowing the

storage of energy. In a 4-level laser, a final level, which is not the ground state, is used. The basic diagram is shown in the left-hand part of Fig. 8.9.

Fig. 8.9 here

Suitable energy-level diagrams of this general type can be found, particularly for ions of the rare earth elements. The ions can be incorporated into certain crystals such as CaF_2 or $CaWO_4$, and also in glass. It is important that level 3 (the storage level) has a comparatively long lifetime so that the ions can be accumulated there. On the other hand, level 4 must be depopulated efficiently. In many elements level 4 is so close to the ground state that cooling is necessary to reduce its thermal population. Laser action has been achieved for most of the rare earth ions. An especially useful type of 4-level laser is the Nd:YAG laser, for which Nd^{3+} ions have been incorporated into an ytterbium-aluminum host crystal of garnet type ("Ytterbium-Aluminum-Garnet", $Y_3Al_5O_{12}$). The lasing transitions for this laser are shown in the centre of Fig. 8.9; in particular, the most commonly used one at 1.064 μm. In the right-hand part of the figure a frequently used Nd:YAG laser arrangement with two linear flashlamps in a bi-elliptic pumping cavity for efficient pumping of the rod is shown. Nd:YAG lasers with a high output power are constructed with an oscillator followed by one or several amplifier stages. This is a very general construction for pulsed lasers. The oscillator is designed for relatively low power. It is then possible to control the mode structure, linewidth and pulse length precisely. A sharp frequency, a short pulse length and a clean TEM_{oo} mode can generally only be achieved at the expense of the output power. A laser amplifier, consisting of a larger flash-lamp-pumped rod, will boost the energy of the pulse without changing the beam quality. The diameter of the amplifying medium is successively increased in the amplifying stages and the laser beam is correspondingly expanded. The technology of solid-state lasers is discussed in Refs [8.22-24]. High-power Nd lasers are used in fusion research based on laser-driven inertial confinement [8.25-8.27].

A typical Nd:YAG laboratory laser system for spectroscopic applications is an oscillator-amplifier arrangement yielding 1.06 μm pulses of 10 ns duration and 1 J energy at a repetition rate of 10 Hz. In such systems, a so-called unstable resonator (See Fig. 8.4) is frequently used to allow a more efficient energy extraction from the oscillator rod than that which is possible for a resonator sustaining a TEM_{oo} mode. Instead of a semi-transparent output coupler a very small central feedback mirror is used and the output power is extracted in an annulus around this mirror. In rod arrangements, Nd:Glass is limited to very low repetition rates because of the poor thermal properties of glass, leading to strong lens effects. However, by using a slab arrangement instead of a rod for the active medium, as illustrated in Fig. 8.10, lensing effects can be shown to self-compensate and it is possible to construct very efficient glass lasers [8.28]. The Nd:YAG and glass materials absorb

Fig. 8.10 here.

Fig. 8.11 here

the pumping radiation mainly in the red spectral region, as shown in Fig. 8.11. New host materials, such as GGG (Gadolinium-Gallium-Garnet $Gd_3Ga_5O_{12}$) and GSGG (Gadolinium-Scandium-Gallium-Garnet), better utilize the available radiation and show great promise. Different laser crystals are described in Ref. [8.24]. Increased efficiencies (beyond the 2% wall-plug power to laser power efficiency typical for a Nd:YAG laser) are attainable by pumping a YAG rod with a suitable frequency-matched diode laser (See p. xxx) [8.29]. In Fig. 8.12 the pumping of a miniature rod is shown yielding single-mode output at an efficiency of up to xx per cent. Such a laser is ideal as a high-quality oscillator for subsequent amplification. As high-power diode lasers become available at reduced prices, high-power solid-state lasers not employing flash-lamp technology will emerge.

Fig. 8.12 here

8.4.3 Pulsed Gas Lasers

The lasers we have considered so far have a solid material as the active medium. Generally, flash-lamp pumping is employed and short pulses are obtained at a repetition rate of typically 10 Hz. High peak powers are obtained in the Q-switched mode (MW-GW). Gaseous

media can also be used for the generation of short laser pulses. We shall here consider the nitrogen laser, the excimer laser and the copper vapour laser. The relevant parts of the N_2 molecule level diagram and the basic arrangement for the N_2 laser are given in Fig. 8.13. Pumping is achieved using an electrical discharge of short

Fig. 8.13 here

duration, transversely, in a tube through which N_2, at a pressure of about 100 torr, is flowing. Recently, sealed N_2 lasers of low power have become available. The transfer probability at electron impact for X→C is much larger than for X→B. Thus, population inversion occurs at level C with regard to B. However, the lifetime of state C is only about 40 ns, whereas the corresponding value for state B is about 10 μs. A very fast discharge, generated using a Blumlein circuit is utilized, since the upper level cannot store energy (Q-switching is not possible). The population inversion can obviously be achieved only for a short time (self-terminating transition). The pulse length for the nitrogen laser is normally less than 10 ns and the emission follows at 337.1 nm. Peak powers up to 1 MW can be achieved. Pulse energies are typically a few mJ, and repetition rates exceeding 100 Hz can be obtained. The nitrogen laser has such a high gain that a laser beam can be obtained even without cavity mirrors through amplified spontaneous emission (sometimes the term super-radiant laser is used). Normally a totally reflecting mirror is used at one end of the gain tube while the window at the opposite end has a very high transmission. The divergence of the beam is given by the geometry of the discharge channel and is typically 10 mrad.

The construction of an excimer laser [8.30-8.32] is similar to that of an N_2 laser. Excimer molecules ("excited dimers") are characterized by the absence of a stable ground state while short-lived, excited states exist. In excimer lasers molecules such as KrF and XeCl are used as the active medium. These molecules are found in the excited state in a fast, electrical discharge in a mixture of the inert gas and F_2 or HCl (Cl_2). The high reactivity of the latter gases makes material selection, gas handling etc. critical for this type of laser. In Fig. 8.14 an excimer level diagram and laser

Fig. 8.14 here

lines for different excimer molecules are given. Since no ground state exists excimer molecules constitute the perfect laser medium with automatic population inversion once a molecule has been created. Important laser emission lines are 249 nm (KrF; yields the highest power) and 308 nm (XeCl, best suited for dye laser pumping). Pulse energies of hundreds of mJ can be achieved and average powers of 100 W can be approached. Excimer laser technology is quickly maturing, and these lasers find many important applications.

Pulsed CO_2 lasers, which were available long before excimer lasers, have a similar construction. These infra-red lasers are of great technological importance. CO_2 lasers will be discussed later.

In the copper vapour laser the discharge tube must be heated to high temperatures in order to produce a sufficient Cu vapour pressure. This laser emits at 510 and 578 nm corresponding to the ($4p\ ^2P_{3/2}$ - $4d\ ^2D_{5/2}$) and ($4p\ ^2P_{1/2}$ - $4d\ ^2D_{3/2}$) transitions, respectively. Since the terminal ^2D states are metastable only pulsed operation is possible. High repetition rates can usually be obtained with this laser, up to 10 kHz. The average power can exceed 10 W. Exchanging copper for gold results in red emission at 628 nm.

Whereas population inversion can often be achieved relatively easily with a pulsed pumping source, it is considerably more difficult, and sometimes impossible, to continuously maintain population inversion while laser action prevails. Clearly, lasing means that excited atoms decay with the emission of stimulated radiation and thus the laser action itself will cause the lasing action to stop. Clearly, efficient pumping mechanisms are required. We will now study some important types of continuous fixed-frequency lasers which all work with gaseous laser media.

8.4.4. The He-Ne Laser

The helium-neon laser was the first gas laser and it was designed and built by Javan and co-workers [8.33] shortly after the introduction of the ruby laser. The He-Ne laser is the most common of all

laser types. The construction can be made comparatively simple and cheap, and continuous laser action is obtained. The active medium is a gas mixture of He and Ne (ratio 5:1) in a glass tube at a total pressure of about 1 torr. Energy is added through an electric discharge through the gas. In order to understand the principle of the He-Ne laser, the energy level diagrams of both He and Ne must be considered. (Fig. 8.15). In the discharge (1000 V, 10 mA) He atoms

Fig. 8.15 here

are excited to the metastable 2 $^3S_1$ and 2 $^1S_0$ states through electron impact. In Ne the 2s and 3s level systems have almost the same energies as the metastable He states. Because of this, the probability of Ne excitation through collisions with metastable He atoms is very large. A population inversion between the s states and the lower-lying 3p and 2p levels is achieved and several laser transitions are possible. Since the lifetimes of the p states are very short (~10 ns) in comparison with the s state lifetimes (~100 ns), the population inversion can be maintained and continuous lasing is achieved. The reflection properties of the laser mirrors determine which line will lase. The most frequently used line is the red line at 6328 Å. The Doppler width of this line is about 1700 MHz. With a typical resonator length of 30 cm a mode separation of 500 MHz is obtained. Such a laser will exhibit 2 or 3 modes. With a sufficiently short laser (10-15 cm), single-mode operation can be attained. He-Ne lasers yield low output powers, typically a few mW.

Primary energy storage in He is also used in the helium-cadmium laser. Here, a sufficient metal vapor pressure must be achieved by heating. Excited Cd ions are produced by Penning ionization:

$$A^* + B \rightarrow A + B^+ + e$$

Two short-wavelength lines, 4416 Å ($4d^95d\ ^2D_{5/2} - {}^2P_{3/2}$) and 3250 Å ($4d^95d\ ^2D_{3/2} - {}^2P_{1/2}$), are obtained at power levels of 50 and 5 mW, respectively. An alternative way of producing the excited Cd ions is to use soft X-ray photo-ionization of ground-state $4d^{10}4s$ Cd atoms [8.34]. High-power laser pulses impinging on a high-Z material, such

as Ta, can be used for soft X-ray production (See p. xxx). Using soft X-ray pumping gain has also been demonstrated in In III (185 nm) [8.35] and Xe III (109 nm) [8.36].

8.4.5 Gaseous Ion Lasers

In gaseous ion lasers a population inversion between excited states of ionized argon or krypton is achieved. The pumping is accomplished through a strong DC discharge in low-density gas (~0.2 torr). The discharge tube is 1-2 m long and current densities of about 500 A/cm^2 are used. Thus, a high electrical power is needed (~10 kW) and the discharge tube, which is made of beryllium oxide or graphite, must have an efficient water cooling system. Excited ions are produced in collisions between inert gas atoms and electrons. For ionization of an argon atom an energy of 15.75 eV is needed. The interesting excited ionic states belonging to the configuration $3p^44p$ are located about 20 eV above the ionic $3p^5$ ground state. In Fig. 8.16 a partial level scheme for Ar^+ is given, with laser lines

Fig. 8.16 here

connecting $3p^44p$ levels and $3p^44s$ levels indicated. Several blue and green laser lines are obtained (5145, 5017, 4965, 4880, 4765, 4727, 4658, 4579 and 4545 Å). The strongest lines are

$$5145\ \text{Å} \quad 3p^44p\ {}^4D_{5/2} \rightarrow 3p^44s\ {}^2P_{3/2}$$

and

$$4880\ \text{Å} \quad 3p^44p\ {}^2D_{5/2} \rightarrow 3p^44s\ {}^2P_{3/2}$$

When using laser mirrors with a high reflectivity in the blue-green region all the lines are produced simultaneously. Argon-ion lasers with a total output power of up to 40 W are commercially available. In Fig. 8.17 the principle arrangement of an argon-ion laser is shown. By using a prism in front of the totally reflecting mirror the individual spectral lines can be isolated. For a certain position of the prism only one wavelength is reflected back towards the semi-transparent output coupler, while the other wavelengths are

refracted out of the cavity. By introducing an intracavity solid Fabry-Pérot interferometer (etalon), single-mode oscillation can be obtained.

Fig. 8.17 here

At very high discharge currents laser transitions are also obtained in doubly ionized argon. Two UV lines, at 3511 and 3638 Å, are then obtained with powers of up to 3 watts.

The krypton-ion laser has the same construction as the argon-ion laser but the discharge tube is instead filled with krypton. Apart from blue and green lines, several red lines are also obtained with this laser (7931, 7525, 6764, 6471, 5682, 5309, 5208, 4825, 4762, 4680, 4131 and 4067 Å), as well as strong UV lines (3564, 3507 and 3375 Å). Ion lasers are discussed in greater detail in Ref. [8.37].

8.5 Tunable Lasers

Whereas fixed-frequency lasers have found important applications in e.g. measurement techniques, information transmission, holography and material processing, tunable lasers are of greatest interest for atomic and molecular spectroscopy. Using different types of tunable lasers the wavelength range 320 nm to tens of μm can be covered by direct laser action, and the tunability region of an individual laser can be considerably extended using non-linear optical effects. Tunable lasers comprise dye lasers, F-centre lasers, certain solid-state lasers, spin-flip Raman lasers [8.38], parametric oscillators, high-pressure CO_2 lasers and semiconductor lasers. Here we will discuss the most important of these laser types. Overviews of tunable lasers can be found in Refs [8.39-41].

8.5.1 Dye Lasers

Laser action in organic dyes was discovered independently by Sorokin et al. [8.42] and Schäfer et al. [8.43] in 1966. Since then, several hundreds of dyes have been shown to have suitable properties, to greater or lesser degrees, for use as laser media. One of the most

common laser dyes is Rhodamine 6G dissolved in methanol or ethylene glycol. The complex structure of organic dyes is illustrated in Fig. 8.18, where the formula for Rhodamine 6G is shown.

Fig. 8.18 here

Fig. 8.19 here

The general energy-level structure of an organic dye is shown in Fig. 8.19. The transitions relevant for laser action occur between the two lower electronic singlet states. The ground state, as well as the excited state, is split into a continuous structure of smeared energy sublevels due to the interaction with the solvent. Normally the molecules are Boltzmann-distributed on the lowest sublevels of the ground state. The molecules can be excited to the next singlet band with light. In radiationless transitions the molecules relax very quickly ($\sim 10^{-12}$s) to the lowest level of the excited state, from where the molecules return to the sublevels of the ground state with a time constant of about 10^{-9}s, emitting fluorescent light. The resulting absorption and emission curves for Rhodamine 6G are included in Fig. 8.19. Because of the relaxation in the excited singlet band the same fluorescence curve is obtained regardless of the spectral distribution of the absorbed light. For example, the curve given in the figure is obtained regardless of whether a flash-lamp or a fixed-frequency laser is used for the excitation.

The usefulness of an organic dye for laser applications much depends on the position of higher-lying singlet bands, and on the influence of the system of triplet levels that is always present in organic dye molecules. If a higher-lying singlet state has an inappropriate energy, a strong absorption of fluorescence light results. Through radiationless transitions, excited dye molecules can be transferred to the triplet system. If a large number of molecules assemble in the lowest triplet state, the fluorescent light from the singlet system can be strongly absorbed by triplet molecules. If the organic dye is pumped sufficiently strongly, a population inversion between the lowest sublevel of the upper singlet state and the sublevels of the ground state is obtained. Amplification by stimulated emission can then be achieved. If a dye solution is contained in a cell,

placed in a laser cavity, and sufficient pumping power is supplied, laser action will occur (Fig. 8.20). With broadband laser mirrors stimulated emission is obtained in a wavelength range of a few tens of Å close to the peak of the fluorescence band.

Fig. 8.20 here

A very important step was taken by Soffer and McFarland [8.44] in 1967 by replacing the totally reflecting mirror with a grating in a Littrow mount (p. xxx). A frequency-selective feedback was obtained and the band width of the stimulated radiation was reduced to about 0.5 Å. By turning the grating the laser could be continuously tuned over the fluorescence band of the dye. In Fig. 8.20 an arrangement for flash-lamp-pumping of a tunable dye laser is shown. Here, a tube is used for the dye solution which is pumped with a linear flash-lamp. Laser pulses with a duration of about 1 μs and a peak power of several kW are obtained. The repetition rate is generally about 1 Hz. Pulsed dye lasers are more frequently pumped by a fixed-frequency laser, normally a nitrogen, an excimer, a copper or a frequency-doubled Nd:YAG laser (See p. xxx, p. xxx and p. xxx). In Fig. 8.21 three different arrangements are shown. In the Hänsch design [8.45], an intracavity beam expander is used to widen the diameter

Fig. 8.21 here

of the beam so that more lines of the Littrow-mounted grating are illuminated. This leads to an increased resolution (p. xxx) at the same time as the grating is protected from local heating. The linewidth with such an arrangement is typically 0.1 Å. Using an intracavity etalon the linewidth can be reduced by a factor of 10. Instead of using a telescope a multiple-prism arrangement can be used, since expansion across the rulings is the only consideration from a resolution point of view. Note that because of the short pumping time (5-10 ns) there is no time for a cavity mode structure to build up in a short-pulse laser. Mode positions are only weakly indicated in the essentially smooth frequency distribution.

In Fig. 8.21 an arrangement is shown in which all the grating lines can be utilized without using any form of beam expansion [8.46]. Here, grazing incidence on a fixed grating is employed. The laser is

tuned by turning a mirror reflecting the first order of the grating back on itself. The useful laser beam can be taken out as the zeroth order beam from the grating (reflection) or through a partially transmitting end mirror. The latter arrangement reduces the broad-band dye emission. By exchanging the turning mirror for a grating in a Littrow mount a still higher resolution can be achieved. By eliminating the telescope the cavity can be made very short. This leads to many round trips during the pulse, a large free spectal range and the possibility of single-mode operation.

If a high pulse energy is needed while retaining a small linewidth and a high beam quality, it is advisable to utilize an oscillator/amplifier arrangement as mentioned above. In Fig. 8.22 two examples

Fig. 8.22 here

are given. In order to achieve a very small linewidth (~100 MHz) ane external Fabry-Pérot interferometer can be used to filter the oscillation output before amplification. In the figure the possibility of pressure-scanning the laser is also illustrated. Since grating, internal and external Fabry-Pérot are tuned in the same way when the pressure is changed (the expression n·1 occurs in all the formulae) all the elements will remain synchronized once they have been correctly adjusted (c.f. the discussion on p. xxx).

Pulsed dye lasers can be operated from 320 to 1000 nm using different dyes. In Fig. 8.23 tuning curves for a dye laser, pumped by an excimer laser, are shown. An energy conversion of 10-20 per cent

Fig. 8.23 here

is usual. With a frequency-doubled Nd:YAG laser (532 nm) the conversion for Rhodamine dyes can exceed 40 per cent. The frequency range of dye lasers can be extended using non-linear optics techniques (p. xxx).

As for fixed-frequency lasers, it is considerably more difficult to achieve continuous laser action than pulsed operation with a dye laser. The first continuous dye laser was designed in 1970 by

Peterson, Tuccio and Snavely [8.47]. A special problem associated with organic dyes is the building up of a population of molecules in the lowest triplet state. For pulsed pumping, laser light can be obtained for a short time before triplet absorption dominates. To achieve continuous laser action absorbing triplet molecules must be removed. Certain chemicals, such as cyclo-octatetraene (COT), are very active in transferring triplet molecules to the ground state without emitting radiation (triplet quenching). An argon- or a krypton-ion laser with a power of several watts is used as a pump source for a continuous dye laser. With Rhodamine 6G, a conversion efficiency of 20 per cent can be achieved in the most favourable wavelength region. However, the efficiency is normally lower. At the present time it is possible to cover with a continuous dye laser. In order to achieve continuous laser action a certain dye must be pumped at a suitable wavelength, for which good absorption occurs. The green, yellow and red regions can be covered by dyes that can be pumped by the blue-green lines of the argon-ion laser. Certain dyes need to be pumped by the violet or red lines from the krypton-ion laser. Blue and violet dyes, e.g. Stilbene, require pumping with the UV lines from an Ar^+- or Kr-laser. In Fig. 8.24 an example of the arrangement of a continuous, tunable dye laser is given. Using focused argon-ion laser light a continuous population inversion is maintained at a point on a quickly flowing flat jet of dye that is ejected through a specially designed nozzle. Ethylene glycol is used as the dye solvent, because of its high viscosity. This arrangement ensures an efficient cooling of the dye.

Fig. 8.24 here

The gain volume is at the focal point of a folded cavity, consisting of two spherical mirrors and a flat output coupler. Tuning is accomplished with a birefringent, so-called Lyot-Öhman filter [8.48]. This consists of one or several crystalline quartz plates mounted at Brewster's angle. The dominant transmission maximum of this filter can be moved by turning the optical axis of the filter with respect to the plane of polarization of the light in the cavity. A band width of about 0.5 Å is obtained from a CW dye laser when only a primary tuning element is used. The width of the filter peak is much larger but the laser will only oscillate close to the transmission peak because of the regenerative nature of laser action. With a typical cavity length of 30 cm a mode separation of 500 MHz is obtained and then several hundreds of modes will oscillate under the gain profile, which is given by the frequency selectivity of the cavity (not by any Doppler broadening as is the case in a gas laser). With an intracavity high-finesse etalon (p. xxx), a single cavity mode can be selected and the resulting frequency width for the outgoing light will be several 10's of MHz. The frequency stability is limited by vibrations etc. With a frequency stabilization system the linewidth can be reduced to less than 1 MHz. Such a system is shown in Fig. 8.25. In order to be able to make a system

Fig. 8.25 here

with etalons work over a wide wavelength region, two low-finesse etalons (broad-band coatings) are used in series. With a 1 mm thick etalon (n=1.5), a free spectral range of 100 GHz is obtained and when operated with a maximum close to a maximum of the Lyot-Öhman filter some 10 modes may lase. Adjacent etalon maxima occur where the filter has a substantially reduced transmission. If an additional, thicker etalon is introduced, having a substantially reduced fine spectral range, say 10 GHz, single-mode operation can be achieved. In Fig. 8.26 the transmission profiles of the different resonator components are shown. In order to achieve a high single-mode power a ring laser cavity is frequently used instead of the usual standing wave linear cavity. This avoids the problem of the linear cavity of high non-utilized gain in the standing wave modes, that ultimately will be utilized by an unwanted second cavity mode, that for high pumping power can no longer be suppressed. Tuning curves for a single-mode dye laser are shown in Fig. 8.27. Dye lasers are discussed in detail in Ref. [8.49], and laser dyes are covered in Ref. [8.50].

Fig. 8.26 here

Fig. 8.27 here

8.5.2 Colour-Centre Lasers

In the near-IR region colour-centre (F-centre) lasers can be used [8.51-52]. These lasers resemble dye lasers with regard to function and construction. Instead of the dye solution a cooled F-centre crystal is used as the active, laser-pumped medium. The colour centre is a defect in a crystal lattice, e.g. KCl. The defect consists of an ion vacancy that has trapped an electron. If impurity ions are close to the vacancy the optical properties are changed. F-centre crystals absorb visible radiation and fluorescence in the near-IR region. Using different crystals, the range 1-3.5 μm can be covered. In Fig. 8.28 F-centre structures, absorption and lasing curves are shown as well as a practical arrangement in a commercial F-centre laser.

Fig. 8.28 here

8.5.3 Tunable Solid-State Lasers

Certain solid-state materials have rather broad gain curves and can thus be tuned over a certain range. This is the case for the Nd:Glass laser, which can be tuned in the region 1.0-1.1 μm. The Alexandrite (Cr^{3+}: $BeAl_2O_4$) and emerald (Cr^{3+}: $Be_3Al_2Si_6C_{18}$) lasers that bear a close resemblance to ruby lasers can, in the same way, be tuned in the regions 730-800 nm and 700 - 850 nm, respectively. These lasers can be pumped directly with a flash-lamp. Finally, the transition element lasers should be mentioned. Co:MgF_2 can be pumped by a simple, non-Q-Switched Nd:YAG laser and yields tunable radiation in the region 1.7-2.3 μm. If the material is instead doped with vanadium, it can be tuned in the region 1.0-1.1 μm. Direct generation of tunable laser radiation without using laser systems for pumping is very attractive. In order to extend the tuning range stimulated Raman scattering can be used (see p. xxx). Tunable solid-state lasers are discussed in Refs [8.53-54].

8.5.4 Tunable CO_2 Lasers

The carbon dioxide laser [8.45] is the most efficient gas laser with a wall plug efficiency of about 10%. It works in the IR region around 10 μm. In numerous applications a non-tuned CO_2 laser is used. However, from a spectroscopic point of view, the fact that it can be line-tuned and continuously tuned at high gas pressures is very useful. In Fig. 8.29 a level diagram and a practical arrangement for a tuned CO_2 laser are shown, together with a diagram of the available lines. The CO_2 molecule has three fundamental modes of

Fig. 8.29 here

vibration (see p. xx). In the mode that corresponds to symmetric stretching (ν_1), the two oxygen atoms move in opposite directions while the carbon atom is stationary. In the bending mode (ν_2), the molecule is bent back and forth. Finally, in the asymmetric stretching mode (ν_3), the oxygen atoms move together while the carbon atom moves in the opposite direction. The vibrational state of the molecule is specified by a set of vibrational quantum numbers (ν_1,ν_2,ν_3), one for each vibrational mode. In the CO_2 laser the level corresponding to asymmetric stretching (001) is populated efficiently by almost resonant collisions with excited molecules of nitrogen that have been added to the CO_2 gas. An electric discharge populates the first excited vibrational level in nitrogen. A strong population inversion with respect to the lower-lying CO_2 states (100) and (020) occurs. In a suitably arranged laser cavity, laser emission can occur in the bands 10.2-10.8 μm and 9.2-9.7 μm using a large number of rotational lines. If no special precautions are taken, lasing of the strongest line occurs , P(20) at 10.59 μm. Using a Littrow-mounted grating other individual P and R branch lines can be chosen. Within every line, fine tuning can be accomplished within about 50 MHz, corresponding to the Doppler width at 10 μm for the CO_2 molecules. By utilizing isotopic molecules, like $^{13}CO_2$, further fixed wavelengths can be chosen. A continuous CO_2 laser of this type normally has an electric discharge along the tube. However, it is also possible to work at high gas pressures (atmospheric pressure and up to 10 atmospheres) if a transverse, pulsed discharge is used (TEA-Transverse Electric Atmospheric) laser; c.f. excimer lasers!). At 10 atmospheres the pressure

broadening is about 2 cm^{-1} (60 GHz) and the individual rotational-vibrational lines that are typically separated by 1-3 cm^{-1} merge. Continuous laser action within the band is then possible. Continuous laser action with a certain tunability can be obtained in waveguide lasers, working at 1 atmosphere pressure. A 1 mm thick capillary tube is used as a wave-guide for the laser radiation.

Non-spectroscopic high-power lasers have been constructed with a continuous output up to tens of kW. Such lasers are used industrially for cutting, welding, hardening, etc. High power pulsed CO_2 lasers are also used for fusion research. CO_2 lasers are discussed in Refs [8.55-56].

Lasers with CO as an active medium can also be constructed. This laser type yields a large number of lines in the region 5.1-5.6 μm. In order to achieve efficient operation the discharge tube must be cooled to low temperatures which complicates practical use. It is simpler to use HF or DF lasers, which give lines in the 2.8-4.0 μm region. Such lasers are examples of chemical lasers for which the active molecules are formed in the discharge tube from the supplied gases H_2/D_2 and SF_6.

As we have seen above, lasing has been achieved for a very large number of atomic and molecular lines. A list of these lines can be found in Ref. [8.57].

8.5.5 Semiconductor Lasers

In 1962 several American researchers discovered, essentially simultaneously, that laser action can be achieved in certain semiconductor diode arrangements. The physics behind this process is different from that discussed so far. However, the fundamental requirement of the creation of a population inversion still exists. A typical diode laser material is gallium arsenide, GaAs, which has been strongly doped. Laser action occurs in the transition zone between p- and n-doped material in a diode subject to a voltage applied in the forward direction. In Fig. 8.30 the basic energy-level diagrams for the cases of voltage on and off are shown. The voltage forces

Fig. 8.30 here

electrons as well as holes to the transition region. Here the conduction-band states have excess population with respect to the empty states of the valence band. Stimulated light emission with a photon energy corresponding to the band gap will result upon the recombination of electons and holes. Semiconductor lasers are very small; with typical dimensions of less than one mm. In Fig. 8.31 the geometry of a typical laser diode is shown. Two opposite sides

Fig. 8.31 here

Fig. 8.32 here

are polished and serve as a cavity. Due to the smallness of the cavity, single-mode oscillation is frequently obtained. Diode lasers with an external cavity can also be used.

Semiconductor lasers can be used in the red and particularly in the IR spectral region. Most materials must be cooled for operation, while GaAs diodes can be used at room temperature. The wavelength of the emitted light can be tuned between 800 and 900 nm by changing the temperature. The frequency change is due to a change in the energy gap as well as in the refractive index. Other possibile ways of changing the wavelength of semiconductor lasers include the application of a magnetic field or hydrostatic pressure. Using several materials, generally made up of three elements such as Pb, Sn and Te ($Pb_{1-x}Sn_xTe$) or In, Ga and As ($In_xGa_{1-x}As$), the whole IR region up to about 40 μm can be covered. In Fig. 8.32 the ranges of some diode lasers are shown. Intense research for achieving visible diode laser light is being pursued. Laser diodes can be used in pulsed or continuous operation. A continuous power of hundreds of milliwatts can be obtained from certain diodes. Tunable diode lasers are discussed in more detail in Refs [8.58-60].

Laser diodes have a very high efficiency (up to 80%). Since the light intensity can be modulated very quickly (up to 10^{10} Hz) by voltage variations semiconductor lasers are of great interest for communication. Since the best transmission properties in fibres are obtained at 1.3 μm, great effort has been put into optimizing lasers at this wavelength.

8.6 Non-linear Optical Phenomena

Several non-linear optical phenomena can be utilized for extending the available wavelength range for a certain laser type. First we will consider frequency doubling. In an electric circuit, frequency doubling of an input signal can be achieved by using non-linear components. The corresponding optical phenomenon, which is an example of non-linear optical effects, can be observed in certain crystals that are traversed by very intense laser light. Light propagation through a transparent medium can be considered as a process in which electrical dipoles (electrons bound to a nucleus) are made to oscillate by the radiation field, and thus to re-emit the light. Through interference, light in the beam direction only is obtained. As long as the oscillation amplitude is small the dipoles can follow the applied oscillation, but at higher amplitudes non-linearities occur when the dipoles can no longer reproduce the applied oscillation. Harmonics then occur. If E is the applied electric field and P is the polarization for the optical medium we can write

$$P = \chi^{(1)}E + \chi^{(2)}E^2 + \chi^{(3)}E^3 + \ldots \qquad (8.5)$$

where $\chi^{(i)}$ are polarizability constants (susceptibilities). From the second term in Eq. (8.5.) we obtain for $E=E_o \sin \omega t$.

$$P_2 = \chi^{(3)} E_o^2 \sin^2 \omega t = \frac{1}{2} \chi^{(2)} E_o^2 (1-\cos 2\omega t) \qquad (8.6)$$

This term is responsible for the generation of frequency-doubled light. A prerequisite is that the crystal has a non-central symmetric structure. Using symmetry arguments, it can be shown that for a material with a centre of symmetry all even coefficients $\chi^{(2)}$, $\chi^{(4)}$ etc. must vanish. Since $\chi^{(2)}$ is always small it is necessary for E_o to be sufficiently high. With pulsed lasers electric field strengths of a sufficient magnitude (~ 10^5 V/cm) can easily be obtained so that the terms $\chi^{(1)}E$ and $\chi^{(2)}E^2$ become comparable in magnitude. The generation of frequency-doubled radiation is hampered by wavelength dispersion for the two waves at frequencies ω and 2ω. Since the waves do not normally propagate with the same velocity, destructive

interference occurs with a resulting low yield. By utilizing doubly refractive materials, for which the velocity of propagation for the ordinary ray at ω coalesces with the velocity for the extraordinary ray at 2ω, "phasematching" can be obtained. The phasematching condition also expresses the requirement for conservation of momentum. By tilting the crystal, and thus selecting the direction of propagation through it, phasematching can be achieved within a certain wavelength range. In Fig. 8.33 the generation of a frequency-doubled wave and the achievement of phasematching are illustrated.

Fig. 8.33 here

Temperature also influences the phasematching. It is especially advantageous if phasematching for a direction at 90° to the optical axis can be achieved by temperature adjustment. Then the extraordinary ray is not displaced with respect to the ordinary ray which is otherwise the case, reducing the beam overlap. KDP (potassium dihydrogen phosphate) and KPB (potassium pentaborate) are frequently-used crystals. An energy conversion efficiency of tens of per cent can be achieved for the former material, whereas the latter has a substantially smaller efficiency. Barium-β-borate is emerging as a new high-efficiency material. Because of the non-linear nature of the frequency-doubling process it is normally used in connection with pulsed lasers. Using tunable dye lasers, doubling down to 217 nm can be achieved, with the limit set by material absorption. In Fig. 8.34 frequency-doubling curves for a Nd:YAG-pumped dye laser are given.

Fig. 8.34

By using an intracavity frequency-doubling crystal or an external enhancement cavity [8.61-62] continuous frequency doubling and mixing can also be achieved for CW dye laser radiation. Powers of several mW can then be achieved.

Frequency doubling can be seen as a mixing of two waves of the same frequency in a non-linear medium. The more general processes, sum- and difference-frequency generation are also possible and can be used to generate new frequencies using two lasers. The process can be explained expressing the light field as

$$E = E_1 \cos \omega_1 t + E_2 \cos \omega_2 t \qquad (8.7)$$

The quadratic term can then be written

$$E_2 = \chi^{(2)}[E_1^2 \cos^2 \omega_1 t + E_2^2 \cos^2 \omega_2 t + 2E_1E_2 \cos \omega_1 t \cos \omega_2 t]$$

$$= \chi^{(2)}[\tfrac{1}{2}(E_1^2 + E_2^2) + \tfrac{1}{2}E_1^2 \cos 2\omega_1 t + \tfrac{1}{2}E_2^2 \cos 2\omega_2 t + \qquad (8.8)$$

$$+ E_1E_2 \cos (\omega_1 + \omega_2)t + E_1E_2 \cos (\omega_1 - \omega_2)t]$$

It can be seen, that apart from the doubled frequencies, sum and difference frequencies are obtained. The phasematching is chosen to strongly enhance one of the terms. In Fig. 8.35 curves for sum generation employing a dye laser and harmonics of the Nd:YAG laser are given.

Fig. 8.35 here

For difference-frequency generation materials that are transparent in the IR region are needed. In Fig. 8.36 IR-generation in $LiNbO_3$ (lithium niobate) is illustrated employing single-mode Ar^+ and dye lasers. Crystals of $CdGeAs_2$, $AgGaS_2$ and $AgGaSe_2$ have recently been grown allowing frequency doubling and sum-frequency generation for pulsed CO_2 lasers.

Fig. 8.36 here

The optical parametric oscillator (OPO) process should also be mentioned. Here a non-linear crystal in a cavity is used to generate two new frequencies (ω_1 and ω_2) out of a single one (ω) that is used to pump the crystal. Energy conservation requires $\omega_1+\omega_2=\omega$. The frequency division between the two new waves (the signal and the idler) is chosen by the phasematching condition. The parametric process can also be used in optical parametric amplifiers (OPA). Parametric laser light generation is reviewed in Refs [8.63-64].

Frequency mixing can also be achieved in mixtures of metal vapours and inert gases. Since asymmetry is not present in a gas, terms depending on $\chi^{(2)}$ are excluded. Third-order processes ($\chi^{(3)} \neq 0$) can be utilized. Direct frequency tripling and four-wave mixing processes are of this type. By changing the pressures of the metal vapour and the inert gas, appropriate phasematching for the desired process can be achieved in the presence of anomalous dispersion close to the metal atom lines [8.65]. Degenerate four-wave mixing, where all beams have the same frequency, is a very useful technique for achieving optical phase conjugation [8.66-67]. Widely tunable short-wavelength radiation can be obtained by mixing in inert gases. Tuning curves for non-linear mixing in Xe are shown in Fig. 8.37. Laser spectroscopy in the vacuum ultraviolet (VUV) region is a rapidly growing field. Sources and techniques are discussed in Refs [8.68-71].

Fig. 8.37 here.

Stimulated Raman-scattering processes yield further possibilities. If a gas is irradiated with laser light of sufficiently high power, stimulated Raman scattering occurs. The Stokes-shifted light propagates in the same direction as the pump radiation. In hydrogen gas a vibrational shift of 4155 cm^{-1} (~0.5 eV) is obtained. The process is illustrated in Fig. 8.38 together with an illustration of how higher Stokes components are obtained by further Stokes shifts. Radiation of shorter wavelength can also be obtained (anti-Stokes components) by four-wave mixing between the pump radiation and Stokes-shifted components.

Fig. 8.38 here

A gas pressure of 10 atmospheres is common. There is no phase-matching condition. By using a small number of very efficient dyes in a pulsed dye laser, wavelengths from the vacuum ultraviolet to 10 μm can be achieved by Raman shifting. The efficiency in the conversion to the first Stokes component can exceed 10% whereas higher-order components are much weaker. In Fig. 8.39, the relation between the primary radiation and the generated wavelengths is illustrated. Besides H_2, other gases, in particular D_2 (2987 cm^{-1}) and CH_4 (2917 cm^{-1}), can be used in Raman shifters. Raman shifting is discussed in Ref. [8.72].

Fig. 8.39 here

We will end this section on frequency extension techniques by discussing the CARS (Coherent Anti-Stokes Raman Scattering) process, which is a special case of four-wave mixing [8.73]. The process is useful for the generation of new frequencies (1:st anti-Stokes component in the stimulated Raman scattering discussed above) and also for powerful spectroscopic applications (See p.). In Fig. 8.40 basic diagrams for the process are given illustrating energy and linear momentum conservation.

Fig. 8.40 here

In the CARS process the sample is irradiated by two laser beams and the frequency difference between the beams is chosen to correspond to the vibrational (rotational) splitting of the irradiated molecules. The beams are denoted the pump beam (at frequency ω_p) and the Stokes beam (at frequency ω_S). Two photons of frequency ω_p are mixed with a photon of frequency ω_S, through the third-order susceptibility $\chi(3)$, to generate a stimulated anti-Stokes photon of frequency ω_{AS} (in the anti-Stokes position with regard to the pump beam):

$$\omega_{AS} = 2\omega_p - \omega_S \qquad (8.9)$$

The phase-matching condition can be written

$$\underline{k}_{AS} = 2\underline{k}_p - \underline{k}_S \qquad (8.10)$$

where $\underline{k}$ is the wavevector with $|\underline{k}| = \omega n/c$

In liquids and solids with a strong wavelength dispersion the two primary laser beams must be crossed at a small angle and the generated CARS beam will emerge at still another angle to fulfil the phase matching condition (8.10). In a gas with negligible dispersion (n=1), collinear phase matching is possible. In diagnostic applications, the so-called BOXCARS geometry is frequently used to achieve improved spatial resolution [8.74]. The CARS beam is generated only from the region in which the incoming laser beams cross. In this case two pump beams and one Stokes beam are used.

When the phase-matching condition is fulfilled the power P_{AS} of the generated beam is related to the powers P_p and P_S of the pump and Stokes beams, respectively, through the expression

$$P_{AS} \sim |\chi(3)|^2 \cdot P_p^2 P_S \qquad (8.11)$$

Since $\chi(3)$ is proportional to the molecular number density, N, we make the interesting (and unusual) observation that the generated beam strength is proportional to N^2 rather than to N.

The basis for most non-linear optical processes is discussed in Ref. [8.75]. Several new monographs cover the field extensively [9.76-79].

REFERENCES, CHAPTER 8

8.1 A. Yariv: Introduction to Quantum Electronics, 2nd ed. (Holt, Rinehart and Winston, New York 1976)

8.2 A. Yariv: Quantum Electronics, 2nd ed. (Wiley, New York 1975)

8.3 M. Sargent III, M.O. Scully, W.E. Lamb, Jr.: Laser Physics (Addison Wesley, London 1974)

8.4 O. Svelto: Principles of Lasers, 2nd Ed. (Plenum, New York 1982)

8.5 A.E. Siegman: An Introduction to Lasers and Masers (Mc Graw-Hill New York 1971) New Edition?

8.6 H. Haken: Laser Theory (Springer, Berlin, Heidelberg, New York 1983).

8.7 K. Shimoda: Introduction to Laser Physics, 2nd Ed., Springer Series in Optical Sciences, Vol. 44 (Springer, Berlin, Heidelberg, New York 1984)

8.8 M. Young: Optics and Lasers, 3rd Ed., Springer Series in Optical Sciences, Vol. 5 (Springer, Berlin, Heidelberg, New York 1986)

8.9 L.J. Pinson: Electro Optics (Wiley, New York 1985)

8.10 F.T. Arecchi, E.O. Schulz-Dubois (eds.): Laser Handbook Vol. 1 and 2 (1972); M.L. Stitch (ed.): Vol. 3 (1979); M.L. Stitch, M. Bass (eds.): Vol. 4 (1985); M. Bass, M.L. Stitch (eds.): Vol. 5 (1985) (North Holland, Amsterdam)

8.11 T.H. Maiman, Nature 187, 493 (1960)

8.12 A.L. Schawlow, C.H. Townes: Infrared and Optical Masers, Phys. Rev. 112, 1940 (1958)

8.13 J.P. Gordon, H.J. Ziegler, Ch.H. Townes: Phys. Rev. 99, 1264 (1955)

8.14 C.H. Townes, in Nobel Lectures in Physics, Vol. 4 (Elsevier, Amsterdam 1972)

8.15 N.G. Basov, in Nobel Lectures in Physics, Vol. 4 (Elsevier, Amsterdam 1972)

8.16 A.M. Prokhorov, in Nobel Lectures in Physics, Vol. 4 (Elsevier, Amsterdam 1972)

8.17 D.L. Matthews et al.: Demonstration of a Soft X-Ray Amplifier, Phys. Rev. Lett. 54, 110 (1985)

8.18 S. Suchewer, C.H. Skinner, M. Milchberg, C. Keane, D. Voorhees: Phys. Rev. Lett. 55, 1753 (1985)

8.19 H. Kogelnik, T. Li: Laser Beams and Resonators, Proc. IEEE 54, 1312 (1966)

8.20 A.L. Bloom, Spectra Physics Resonator Paper

8.21 A.G. Fox, T. Li: Resonant Modes in a Maser Interferometer, Bell System Tech. J. 40, 453 (1961)

8.22 W. Koechner: Solid State Laser Engineering, Springer Series in Optical Sciences, Vol. 1 (Springer, Berlin, Heidelberg, New York 1976)

8.23 D.C. Brown: High-Peak-Power Nd:Glass Laser Systems, Springer Series in Optical Sciences, Vol. 25 (Springer, Berlin, Heidelberg, New York 1981)

8.24 A.A. Kaminskii: Laser Crystals, Springer Series in Optical Sciences, Vol. 14 (Springer, Berlin, Heidelberg, New York 1981)

8.25 A.F. Gibson: Lasers for Compression and Fusion, Contemp. Phys. 23, 285 (1982)

8.26 R.S. Craxton, R.L. McCrory, J.M. Sources: Progress in Laser Fusion, Sci. Amer. 255, No.8 (?), 60 (1986)

8.27 N.G. Basov, Yu.A. Zakharenkov, N.N. Zorev, G.V. Sklizkov, A.A. Rupasov, A.S. Shikanov: Heating and Compression of Thermonuclear Targets by Laser Beams (Cambridge University Press, Cambridge 1986)

8.28 J.E. Eggleston, T.J. Kane, K. Kuhn, J. Unternahrer, R.L. Byer: The Slab Geometry Laser, IEEE J. Quant. Electr. QE-20, 289 (1984)

8.29 Opt. Lett. 10, 62 (1985), Opt. Lett. ?, 65 (1985), Opt. Lett. 10, 484 (1985)

8.30 C.K. Rhodes (ed.): Excimer Lasers, Topics in Applied Physics, vol. 30 (Springer, Berlin, Heidelberg, New York 1979)

8.31 M.H.R. Hutchinson: Excimers and Excimer Lasers, Appl. Phys. 21, 15 (1980)

8.32 C.K. Rhodes, H. Egger, H. Plummer (eds.): Excimer Lasers, Conf. Proc. Series No. 100 (American Institute of Physics, New York 1983)

8.33 A. Javan, W.R. Bennet, Jr., D.R. Herriott: Population Inversion and Continous Optical Maser Oscillation in a Gas Discharge Containing a He-Ne Mixture, Phys. Rev. Lett. 6, 48 (1961)

8.34 W.T. Silfvast, J.J. Macklin, O.R. Wood II: High-Gain Inner-Shell Photoionization Laser in Cd Vapor Pumped by Soft X-Ray Radiation from a Laser Produced Plasma Source, Opt. Lett. 8, 551 (1983)

8.35 R. Lacy

8.36 H.C. Kapteyn, R.W. Lee, R.W. Falcone: Observation of a Short-Wavelength Laser Pumped by Auger Decay, Phys. Rev. Lett. 57, 2939 (1986)

8.37 C.C. Davis, T.A. King: Gaseous Ion Lasers, in Advances in Quantum Electronics, Vol. 3 (ed. D.W. Goodwin) (Academic Press, London 1975)

8.38 S.D. Smith, R.B. Dennis, R.G. Harrison: The Spin-Flip Raman Laser, Prog. Quant. Electr. 5, 205 (1977)

8.39 M.J. Colles, C.R. Pigeon: Tunable Lasers, Rep. Prog. 38, 329 (1975)

8.40 A. Mooradian: Tunable Infrared Lasers, Rep. Prog. Phys. 42, 1533 (1979)?

8.41 J. White, L. Mollenauer (eds.): Tunable Lasers, Topics in Applied Physics, Vol. 59 (Springer, Berlin, Heidelberg, New York 1986)

8.42 P.P.Sorokin, J.R. Lankard: IBM J. Res. Dev. 10, 306 (1966)

8.43 F.P. Schafer, W. Smidt, J. Volze, Appl. Phys. Lett. 9, 306 (1966)

8.44 B.H. Soffer, B.B. McFarland: Appl. Phys. Lett. 10, 266 (1967)

8.45 T.W. Hansch: Repetitively Pulsed Tunable Dye Laser for High Resolution Spectroscopy, Appl. Opt. 11, 895 (1972)

8.46 M.G. Littman: Single-Mode Operation of Grazing Incidence Pulsed Dye Laser, Opt. Lett. 3, 138 (1978); S. Saikan: Nitrogen Laser Pumped Single Mode Dye Laser, Appl. Phys. 17, 41 (1978)

8.47 O.G. Peterson, S.A. Tuccio, B.B. Snavely, Appl. Phys. Lett. 17, 245 (1970)

8.48 J. Evans: The Birefringent Filter, J. Opt. Soc. Am. 39, 229 (1949)

8.49 F.P. Schafer (ed.): Dye Lasers, 2nd Ed., Topics in Applied Physics, Vol. 9 (Springer, Berlin, Heidelberg, New York 1978); F.P. Schafer (ed.): Dye lasers, 3rd Edition, Springer, Berlin, Heidelberg, New York 1986).

8.50 M. Maeda: Laser Dyes (Academic Press, Orlando 1984); K. Brackman: Lambdachrome Laser Dyes (Lambda Physik, Göttingen 1986)

8.51 L.F. Mollenauer

8.52 W. Gellerman, K.B. Koch, F. Luty: Recent Progress in Color Center Lasers, Laser Focus 18, 71 (April 1982)

8.53 R.L. Byer (ed): Special Issue on Tunable Solid State lasers, IEEE J. Quant. Electr. QE-21, 1567-1636 (1985). (Papers on Alexandrite, Co:MgF, Ti:AlO and GSGG Lasers)

8.54 P. Hammerling, A.B. Budgor, A. Pinto (eds.): Tunable Solid State Lasers, Proc. of the First International Conference, La Jolla 1984, Springer Series in Optical Sciences, Vol. 47 (Springer, Berlin, Heidelberg, New York 1985)

8.55 D.C. Tyle: Carbon Dioxide Lasers, in D.W. Goodwin (ed.): Advances in Quantum Electronics, Vol. 1 (Academic Press, New York 1970)

8.56 F. O'Neill, W.T. Whitney: A High-Power Tunable Laser for the 9 - 12.5 mm Spectral Range, Appl. Phys. Lett. 31, 271 (1977)

8.57 R. Beck, W. Englisch, K. Gurs: Table of Laser Lines in Gases and Vapors, 3rd Ed., Springer Series in Optical Sciences, Vol. 2 (Springer, Berlin, Heidelberg, New York 1978)

8.58 H. Kressel, J.K. Butler: Semiconductor Lasers and Heterojunction LEDs (Academic Press, New York 1977).

8.59 J.C. Camparo: The Diode Laser in Atomic Physics, Contemp. Phys. 26,443 (1985)

8.60 E.D. Hinkley, K.W. Nill, F.A. Blum: Infrared Spectroscopy with Tunable Lasers, in Ref. (Walter vol 2)

8.61 Intracavity freq. doubling

8.62 B. Couillaud, L.A. Bloomfield, T.W. Hansch: Generation of Continous-Wave Radiation near 243 nm by Sum Frequency Mixing in an External Ring Cavity, Opt. Lett. 8, 259 (1983)

8.63 S.E. Harris: Tunable Optical Parametric Oscillators, Proc. IEEE 57, 2096 (1969)

8.64 Y.X. Fan, R.L. Byer: Progress in Optical Parametric Oscillators, SPIE Vol. 461, 27 (1984)

8.65 P.P. Sorokin, J.A. Armstrong, R.W. Dreyfus, R.T. Hodgeson, J.R. Lankard, L.H. Manganaro, J.J. Wynne: Generation of Vacuum Ultraviolet Radiation by Non-linear Mixing in Atomic and Ionic vapors, in Ref. (Megeve)

8.66 D.M. Pepper: Applications of Optical Phase Conjugation, Sci. Amer. 254, No. 1, 56 (1986)

8.67 H.J. Eichler, P. Gunther, D.W. Pohl: Laser Induced Dynamic Gratings, Springer Series in Optical Sciences, Vol. 50 (Springer, Berlin, Heidelberg, New York 1986)

8.68 T.J. McIlrath, R.R. Freeman (eds): Laser Techniques for Extreme Ultraviolet Spectroscopy (Conf. Proc. Series No. 90) (American Inst. of Physics, New York 1982)

8.69. S.E. Harris, T.B. Lucatorto: Laser Techniques in the Extreme Ultraviolet (Conf. Proc. Series No. 119) (American Inst. of PHysics, New York 1984)

8.70 D.T. Attwood, J. Bokor (eds.): Short Wavelength Coherent Radiation: Generation and Application (Conf. Proc. Series No. 147) (American Institute of Physics, New York 1986)

8.71 C.R. Vidal: Coherent VUV Sources for High-Resolution Spectroscopy, Appl. Opt. 19, 3897 (1980).

8.72 V. Wilke, W. Smidt: Tunable Coherent Radiation Source Covering a Spectral Range from 185 - 880 nm, Appl. Phys. 18, 177 (1979). See also Appl. Phys. 18, 235 (1979)

8.73 J.P. Taran: Coherent Anti-Stokes Raman Spectroscopy, in Ref. (Megeve)

8.74 A.C. Eckbreth: Appl. Phys. Lett. 32, 421 (1978)

8.75 N. Bloembergen: Nonlinear Optics, 3rd Printing (Benjamin, New York 1977)

9.76 Y.R. Shen: The Principles of Nonlinear Optics (Wiley, New York 1984)

9.77 M. Schubert, B. Wilhelmi: Nonlinear Optics and Quantum Electronics, Theoretical Concepts (Wiley, New York 1986)

9.78 V.S. Letokhov, V.P. Chebotayev: Nonlinear Laser Spectroscopy, Springer Series in Optical Sciences, Vol. 4 (Springer, Berlin, Heidelberg, New York 1977)

9.79 M.D. Levenson: Introduction to Nonlinear Spectroscopy (Academic Press, New York 1982)

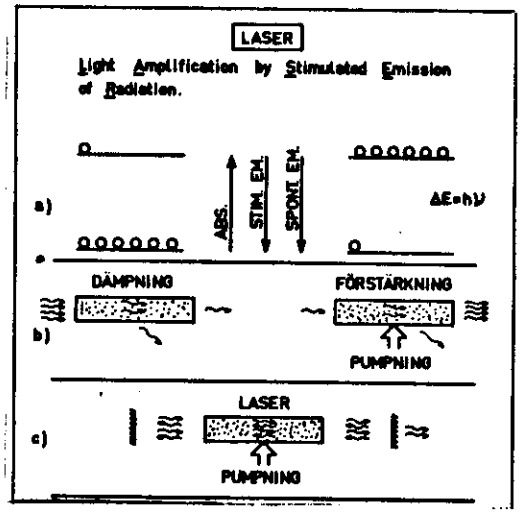

Fig. 8.1 Principle of laser action

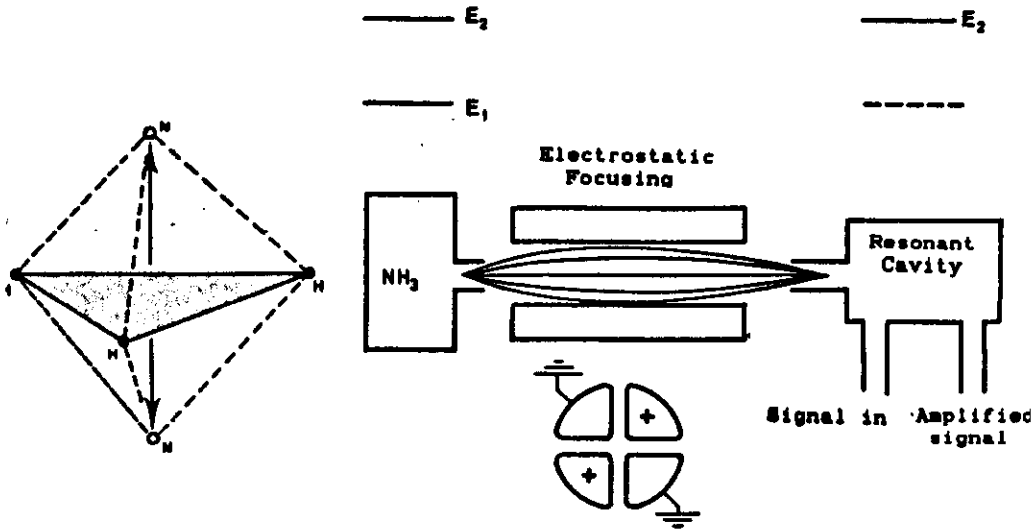

Fig.8.2 The ammonia maser

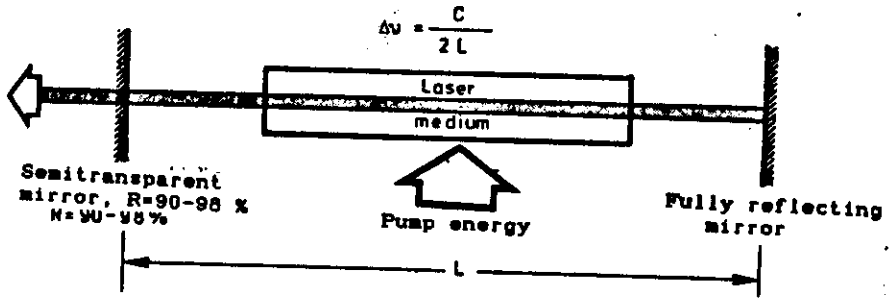

Fig. 8.3 Basic construction of a laser

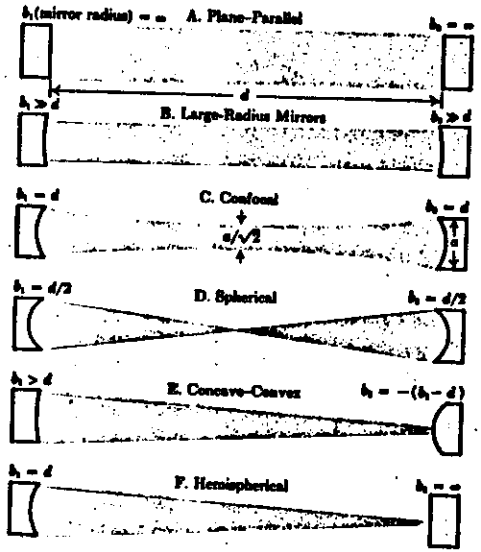

Fig. 8.4 Laser resonators

Figure 2. Resonator Configurations Giving Uniphase Wavefronts
A.L. Bloom, Spectra Physics 1962

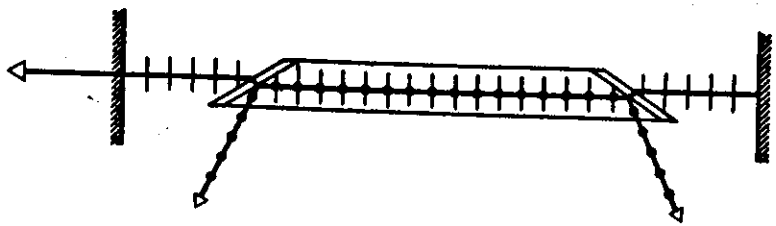

Fig. 8.5 Generation of polarized laser light

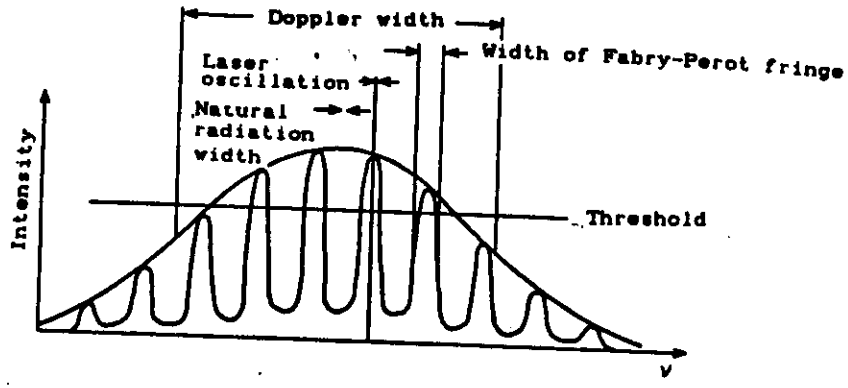

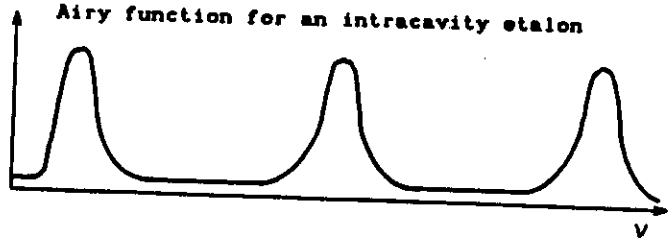

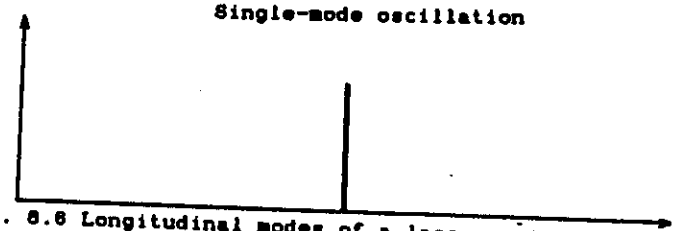

Fig. 8.6 Longitudinal modes of a laser cavity

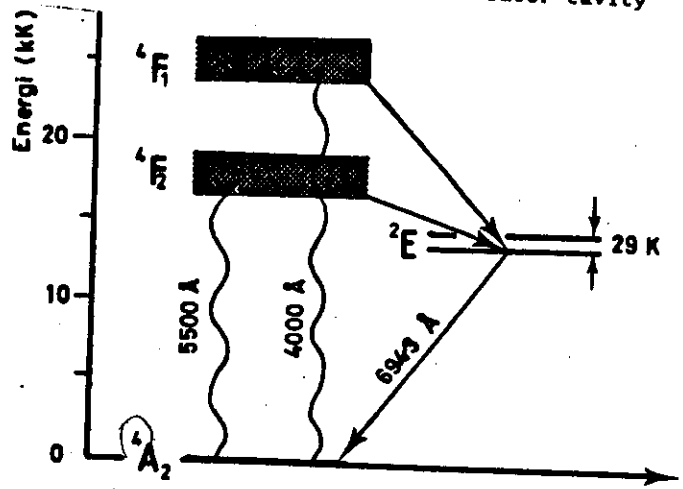

Fig. 8.7 Energy level diagram and absorption curves for ruby

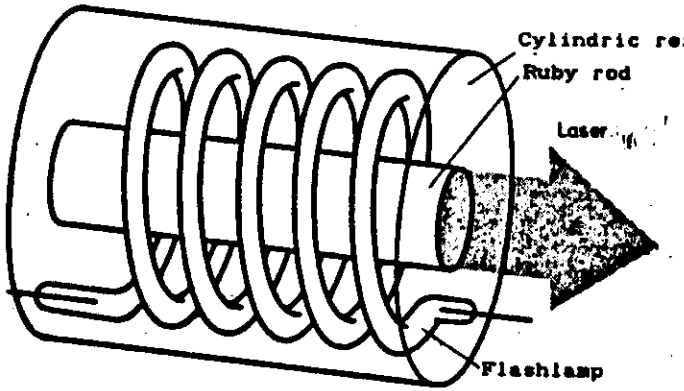

Fig. 8.8 The construction of Maiman's ruby laser

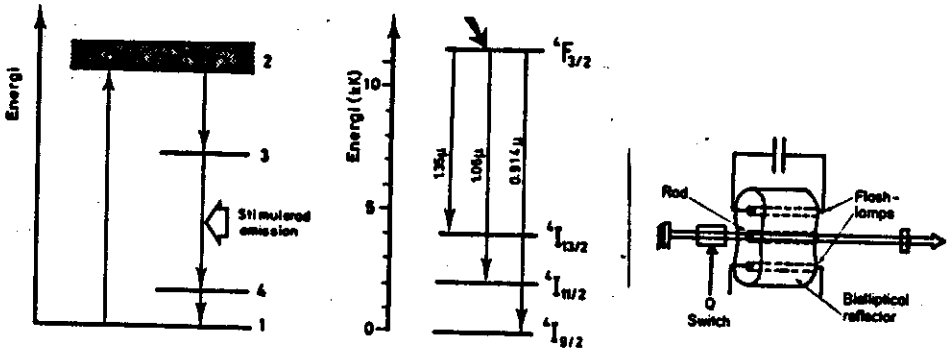

Fig. 8.9 The principle for a 4-level laser (left), transitions in the Nd:YAG material (center) and Nd:YAG laser (right)

297

Fig. 8.10 Gain medium shaped as a slab

Fig. 8.11 Absorption of Nd:YAG crystal

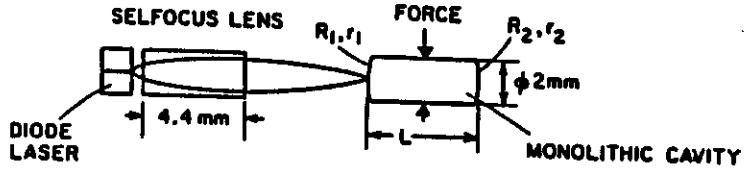

Fig. 8.12 Miniature Nd:YAG laser pumped by a diode laser

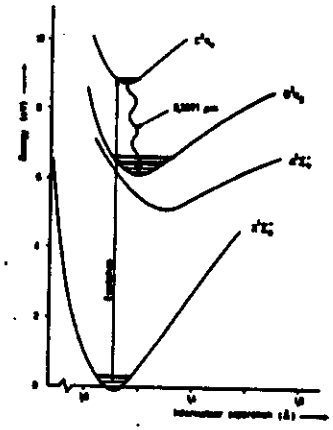

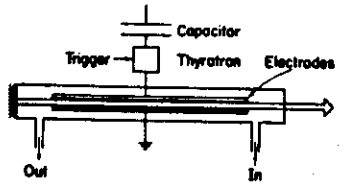

Fig. 8.13 Energy level diagram for N_2 and nitrogen laser arrangement

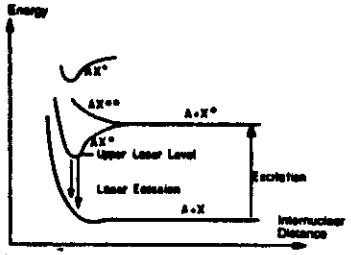

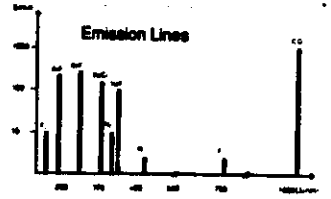

Fig. 8.14 Excimer energy level diagram and excimer emission lines

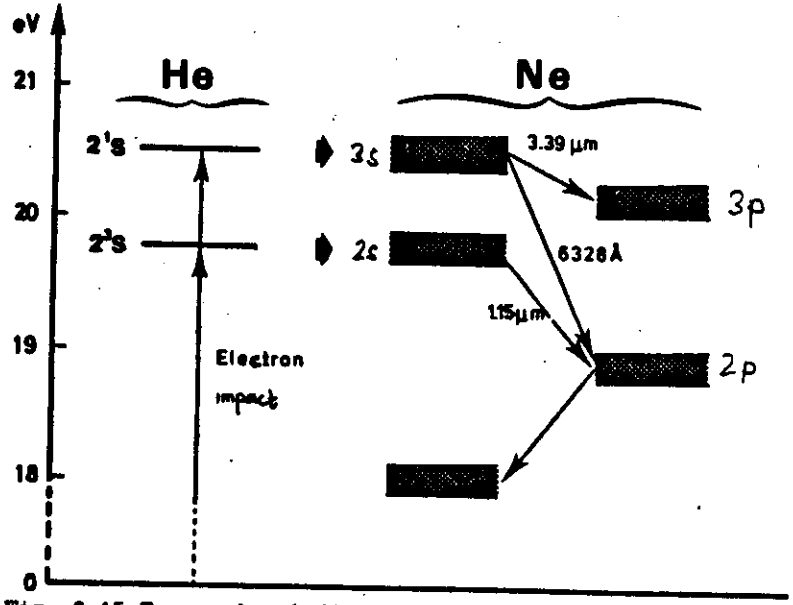

Fig. 8.15 Energy level diagrams relevant to the operation of the He-Ne laser

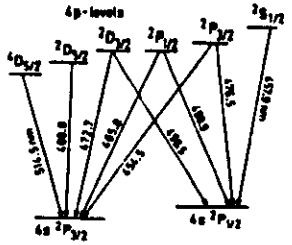

Fig. 8.16 Laser transitions i Ar^+

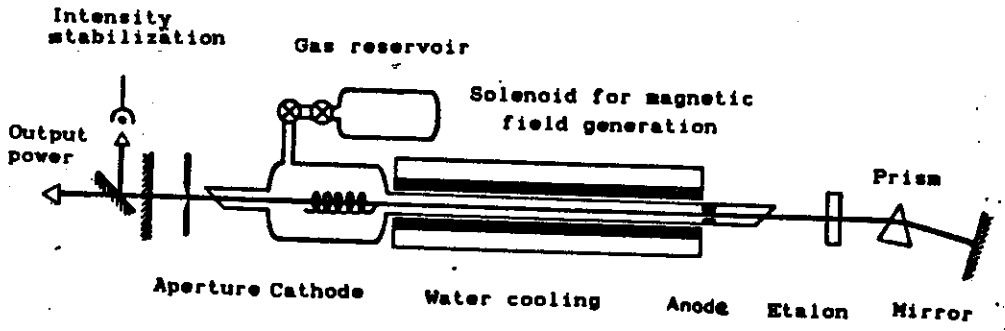

Fig. 8.17 Construction of an argon ion laser

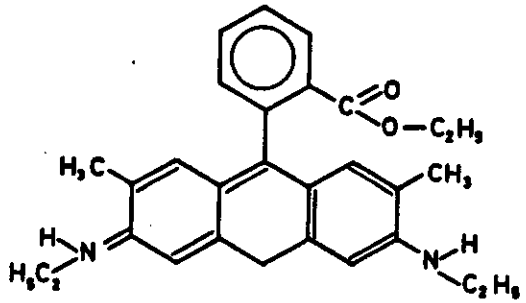

Fig. 8.18 Structural formula for Rhodamine 6G

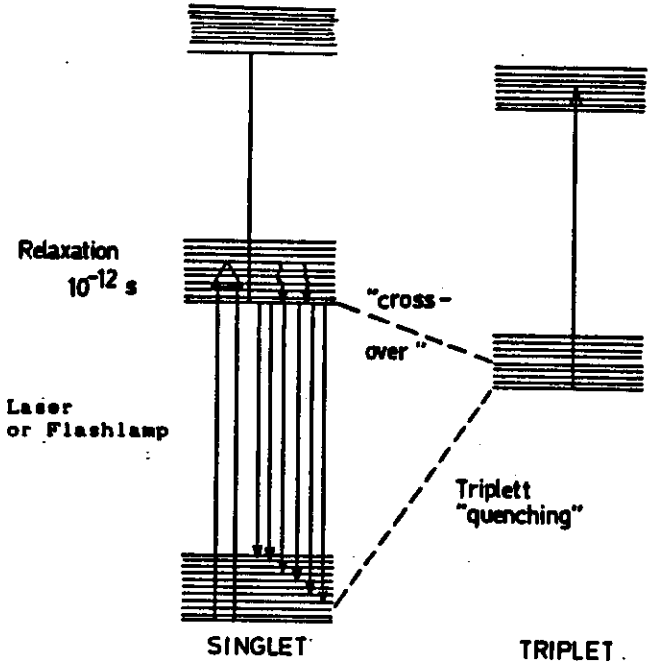

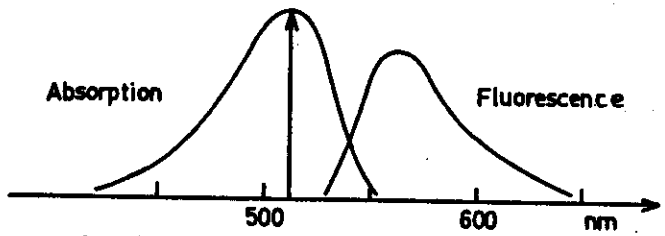

Fig. 8.19 Energy level diagram for organic dyes. Absorption and emission curves for Rhodamine 6G

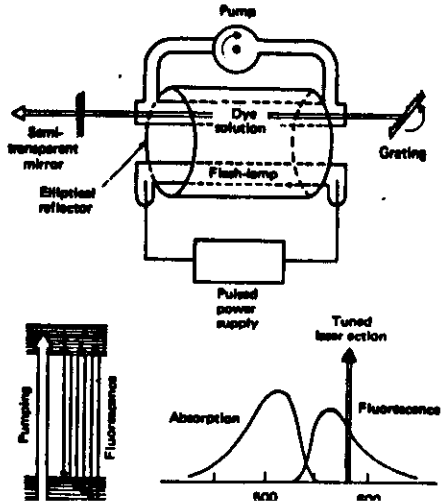

Fig. 8.20 Flashlamp pumped dye laser

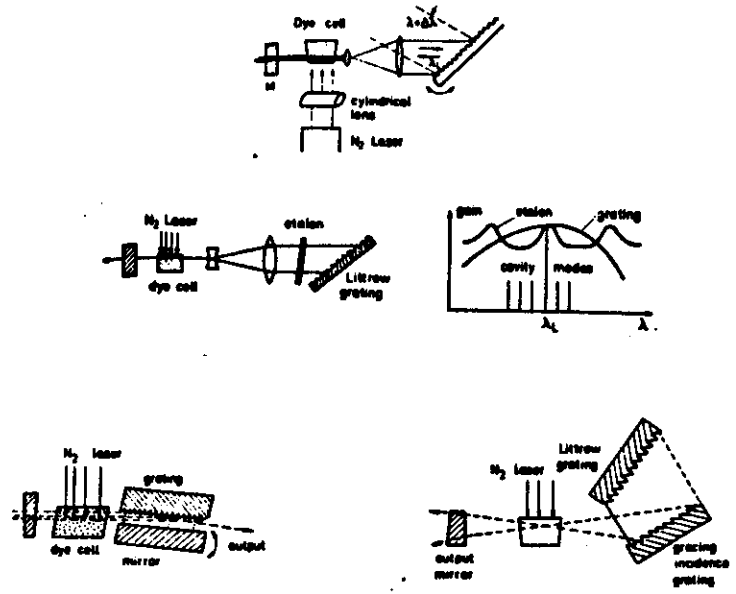

Fig. 8.21 Dye laser cavities

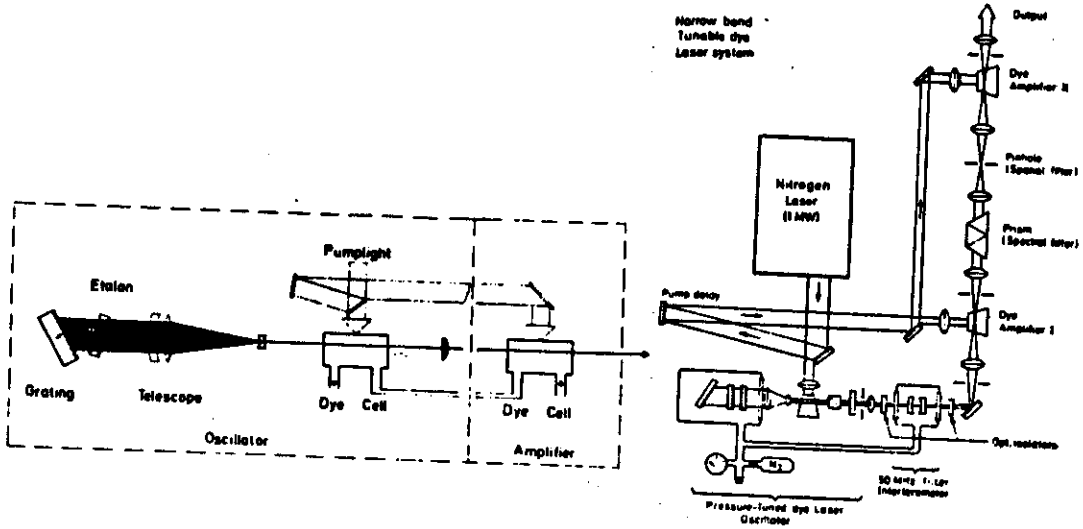

Fig. 8.22 Dye lasers followed by dye amplifiers

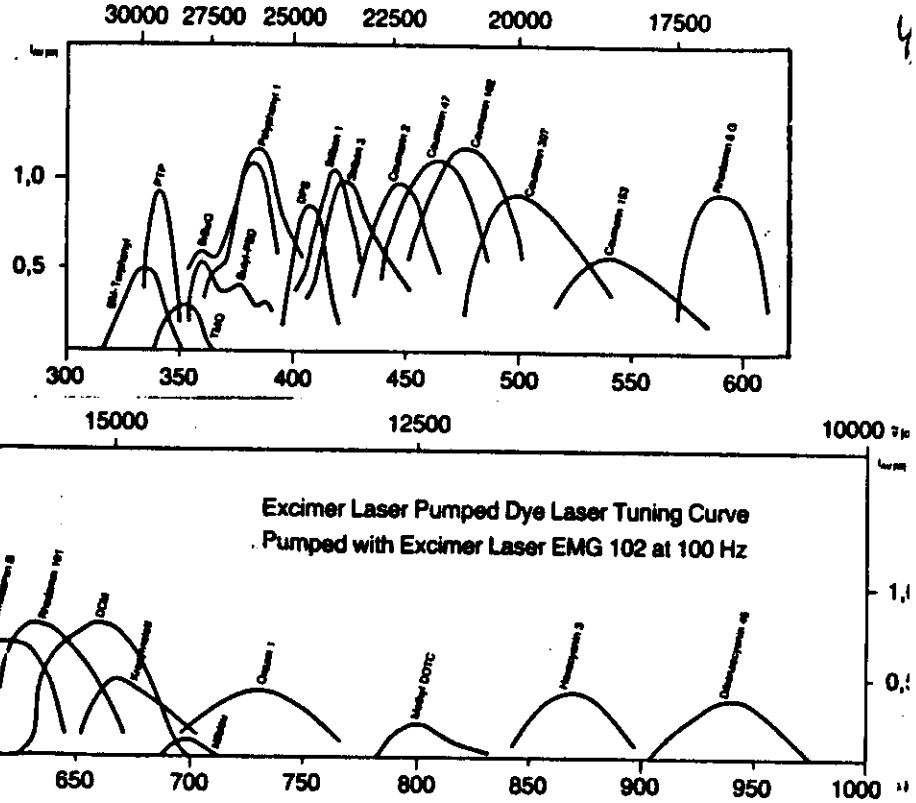

Fig. 8.23 Tuning curves for an excimer-pumped dye laser

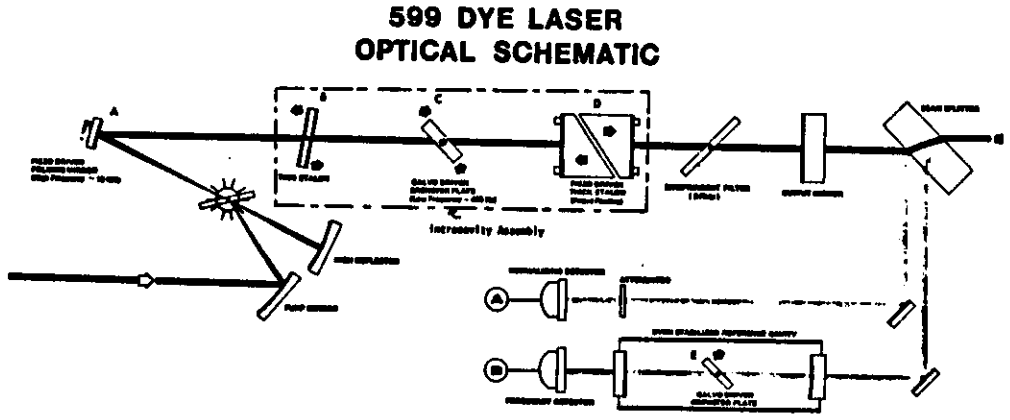

Fig. 8.24 Linear single mode dye laser

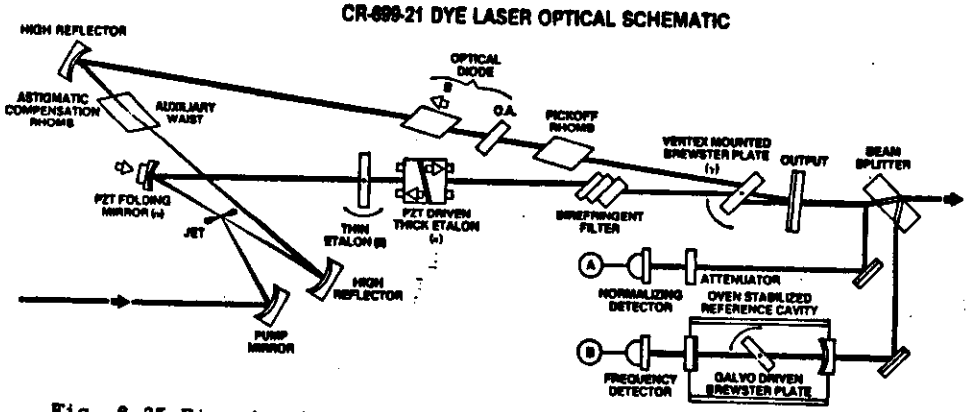

Fig. 8.25 Ring dye laser

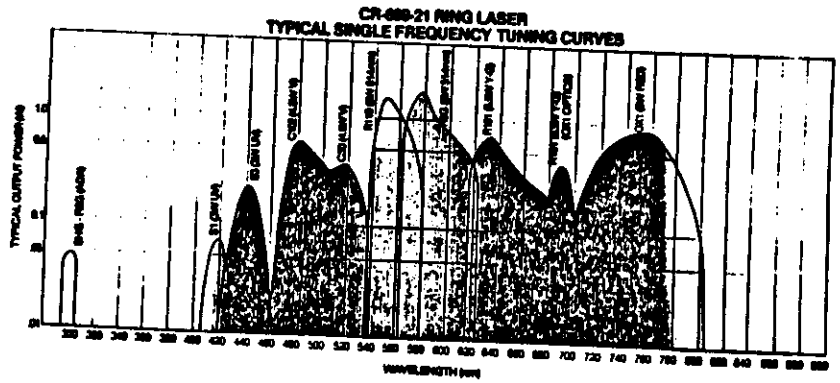

Fig. 8.27 Tuning curves for ring dye laser

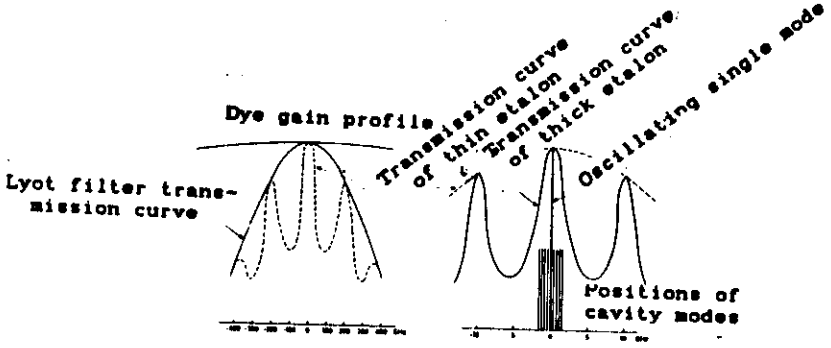

Fig. 8.26 Different transmission profiles pertinent to a linear single-mode dye laser

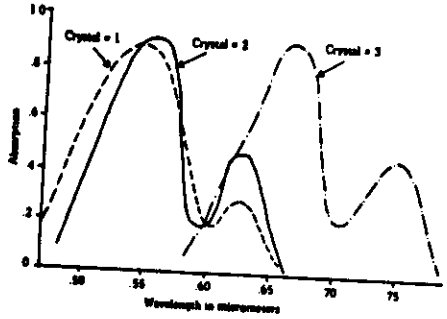

Absorptionskurvor för F-centerkristaller.

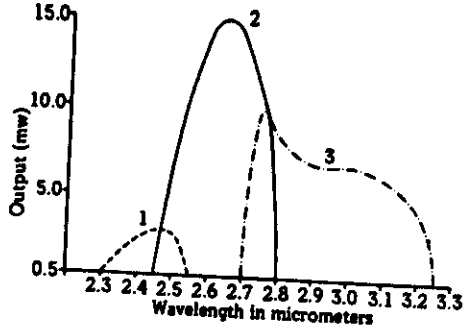

Lasringsområden för F-centra.

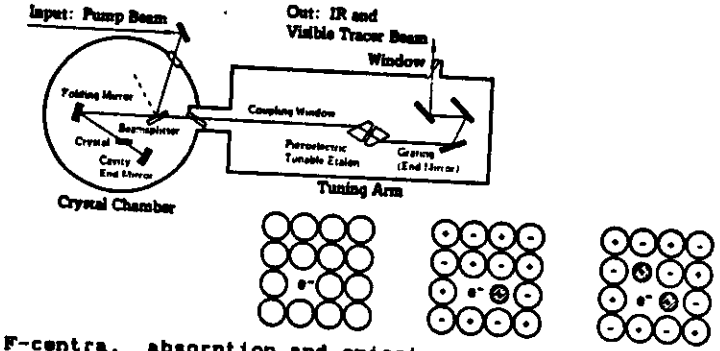

Fig. 8.28 F-centra, absorption and emission curves and F-center laser

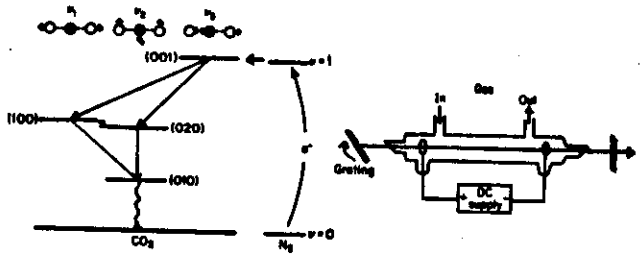

Diagram för CO_2-lasern.

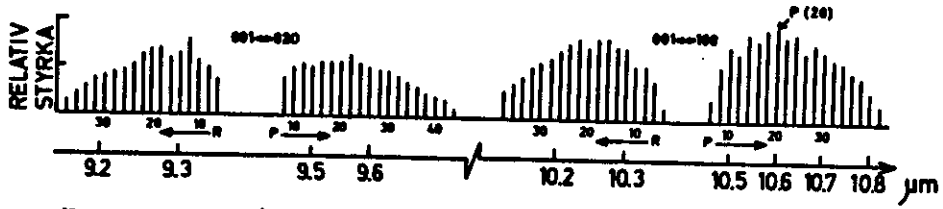

Fig. 8.29 Tunable CO_2 laser

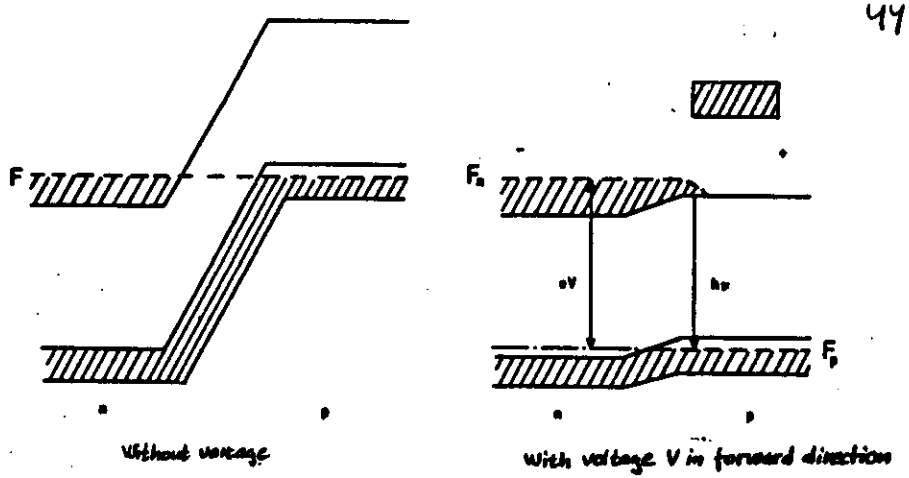

Fig. 8.30 Energy level diagram for diode lasers

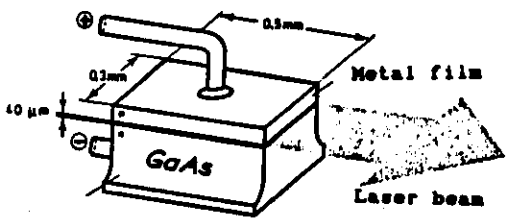

Fig. 8.31 Diode laser

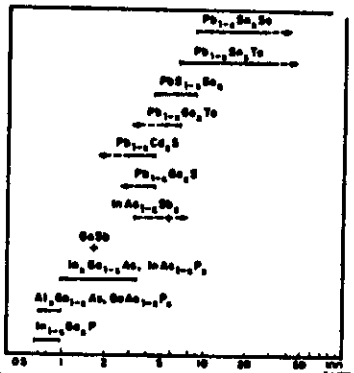

Fig. 8.32 Tuning ranges for different diode lasers

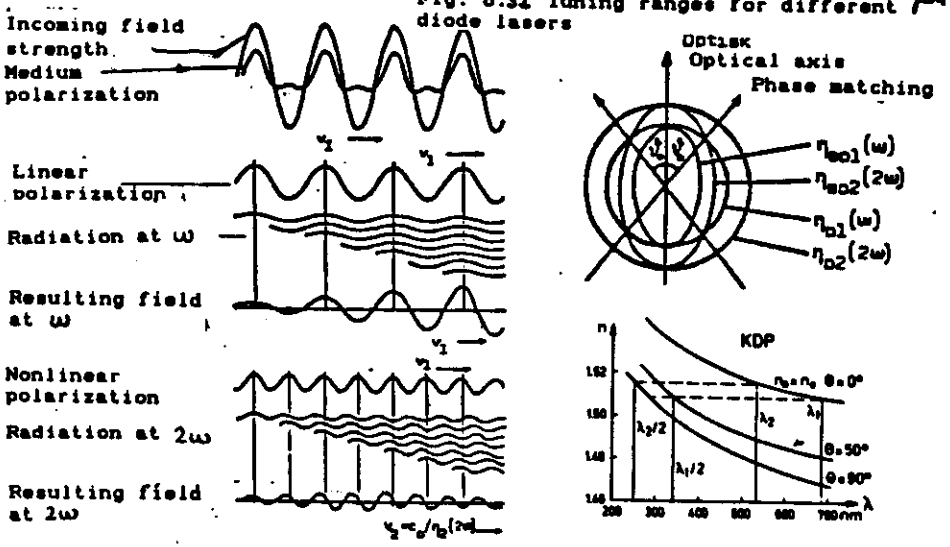

Fig. 8.33 Illustration of phase matching

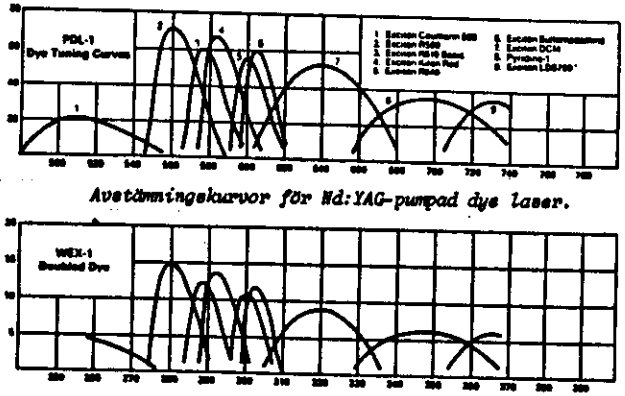

Avstämningskurvor för Nd:YAG-pumpad dye laser.

Fig. 8.34 Fundamental and frequency doubled output of Nd:YAG pumped dye laser

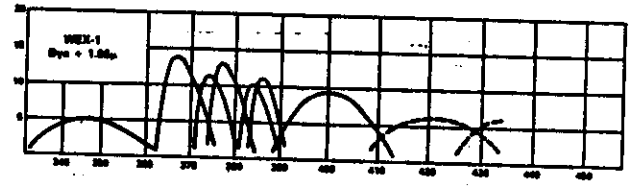

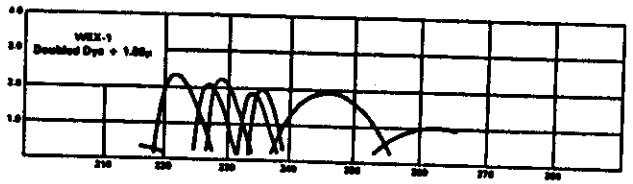

Fig. 8.35 Tuning curves in frequency mixing

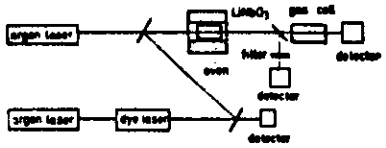

Fig. 8.36 Difference frequency generation between single-mode argon-ion laser and dye laser

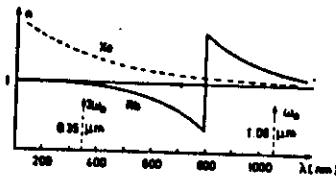

Fig. 8.37 Phase-matched frequency tripling of Nd:YAG radiation in Rb vapour with added Xe

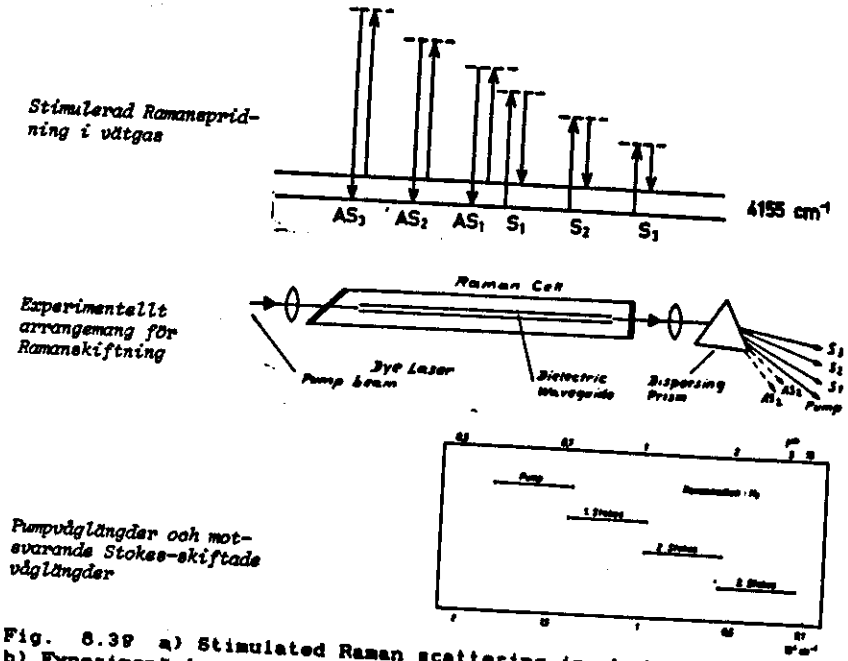

Fig. 8.39 a) Stimulated Raman scattering in hydrogen.
b) Experimental arrangement for Raman shifting
c) Pump wavelengths and corresponding Stokes-shifted wavelengths

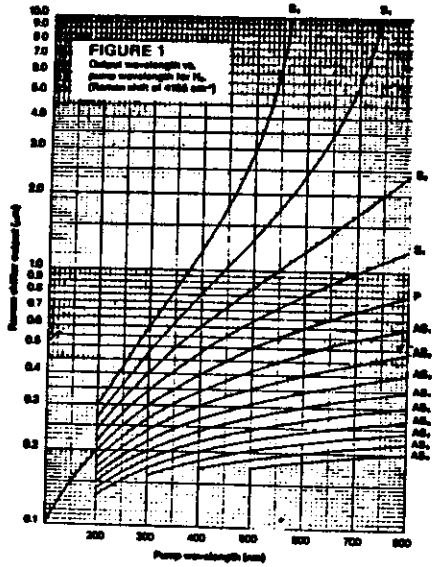

Fig. 8.39 Relation between the primary wavelength and generated wavelengths (H_2, 4155 cm_{-1})

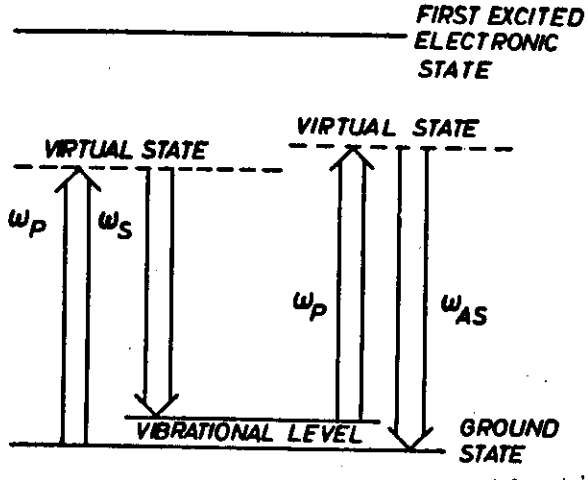

Fig. 8.40 Diagram for CARS

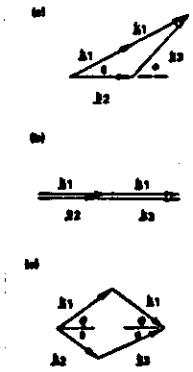

Phase matching condition:
a) dispersive medium
b) collinear
c)BOXCARS geometry